UNIVERSITY OF CALIFORNIA SAN DIEGO

Computational Prediction and Site-directed Mutagenesis Studies of Small Molecule Binding to Fascin

A thesis submitted in partial satisfaction of the requirements for the degree Master of Science

in

Chemistry

by

Aashish Shivkumar

Committee in charge:

Professor Jerry Yang, Chair
Professor Rommie Amaro
Professor Patricia Jennings

2019

The Thesis of Aashish Shivkumar is approved, and it is acceptable in quality and form for publication on microfilm and electronically:

Chair

University of California San Diego

2019

DEDICATION

This thesis is dedicated to Amma, Papa, Abhi, Mama and my grandparents.

EPIGRAPH

The heights by great men reached and kept were not attained by sudden flight, but they, while their companions slept, were toiling upward in the night.

- Henry Wadsworth Longfellow

TABLE OF CONTENTS

LIST OF FIGURES

LIST OF TABLES

LIST OF ABBREVIATIONS

Aβ	Beta-amyloid
ACh	Acetylcholine
AChE	Acetylcholinesterase
AD	Alzheimer's Disease
AMPA	α-Amino-3-hydroxy-5-methyl-4-isoxazolepropionic acid
Amp-100	Ampicillin (100 μg/mL)
APP	Amyloid precursor protein
ASD	Autism spectrum disorder
BSA	Bovine serum albumin
BTA	6-Methylbenzothiazole
CD	Circular Dichroism
CR	Congo Red
DNA	Deoxyribonucleic Acid
DTT	Dithiothreitol
ECL	Enhanced chemiluminescence
EDTA	Ethylenediaminetetraacetic acid
EG	Ethylene glycol
FDA	Food and Drug Administration
FRET	Forster Resonance Energy Transfer
GAP	GTPase activating protein
GEF	Guanine exchange factor
GST	Glutathione S-transferase
GDP	Guanine diphosphate
GTP	Guanine triphosphate
IgG	Immunoglobulin G
IPTG	Isopropyl β-D-thiogalactoside
ITC	Isothermal titration calorimetry
kDa	Kilodalton

L-CPL	Left-handed circularly polarized light
LIMK	LIM kinase
LDS	Lithium dodecyl sulfate
NMDA	N-methyl-D-aspartic acid
nm	Nanometer
PAGE	Polyacrylamide gel electrophoresis
PCR	Polymeric Chain Reaction
PDB	Protein Data Bank
PKC	Protein Kinase C
R-CPL	Right-handed circularly polarized light
RMSD	Root-mean-square deviation
RNA	Ribonucleic acid
ROS	Reactive oxygen species
SDS	Sodium dodecyl sulfate
TBST	Tris buffered saline with Tween 20
ThT	Thioflavin-T
Tris	Tris(hydroxymethyl)aminomethane

ACKNOWLEDGEMENTS

I am indebted to everyone who has been involved in making this thesis possible. I would like to thank my advisor, Professor Jerry Yang, for giving me the opportunity to work in his lab. I am grateful for his support and mentorship. Apart from being a mentor for my project, I am grateful and appreciative of his efforts to help me through the struggles in my personal life. The project that he gave me challenged me on a personal level, and I value the confidence that he had in my ability to conduct independent research. I would also like to thank Professor Rommie Amaro for welcoming me into her lab and giving me the opportunity to learn docking techniques from Zied Gaieb and Conor Parks. I would like to thank Professor Patricia Jennings for believing in me and helping me get over my fear of presenting my research.

I would like to thank Robert Alberstein in the Tezcan group for helping me to acquire Circular Dichroism spectroscopy data. Without this data, I would not have been able to characterize the proteins that I expressed and purified. I am grateful to Zied Gaieb for taking the time to help me interpret the docking results and ITC data.

My lab mates provided invaluable support and advice. I am thankful to those who were already part of the Yang lab when I joined and welcomed me into the lab. Dr. Jessica Cifelli and Kyle Berg worked with me in 6111 when I initially joined. Even though Jessica was busy with her post-doctoral work and Kyle was preparing for his departmental exam, both helped me get started with my research and made me feel comfortable. I would like to give Jessica credit for helping me with my decision to pursue a PhD after I finish my MS degree. She quickly became a role model for me and I knew I wanted to be someone like her in the future. It was a delight to occupy the seat next to Kyle and hear him talk about his love for food, pokemon GO, video games and his amazing family. But apart from all the cool stuff, I would like to thank him for being an amazing mentor.

Whatever I know about protein expression, purification, and most of the techniques, I owe it to Kyle for helping me through each one of them. On the other side in 6213, Dr. Geoffray Leriche, Richard Niederecker and Kristine Teppang made me feel warm and welcomed. Geoffray and I often talked about football in general, about our life experiences and about coming to the US from different countries. I loved watching Champions League games in the middle of the day in the lab. I want to sincerely thank Geoffray for his time and inputs on ITC. It was a struggle and I am grateful for your guidance. Meihan Li was the first person in lab that I became close friends with. We instantly had a connection and helped each other through the first year of grad school. I am grateful to her for being my pillar of strength during the tough times and my partner in crime during my happy moments in lab. I am indebted to her for all the car rides, accompanying me for late night experiments in lab and trying different restaurants and boba places. I am grateful to Meihan, Kristine and Geoffray for their patience and help with my practice talks and inputs for my presentation. I would also like to acknowledge John Kim for his feedback and comments during group meetings and in general for his cheerful nature. I had a blast every time I had a chance to grade finals with him (I always come prepared – takes out three bottles of diet coke).

Serving as a teaching assistant was one of the best experiences I had as a grad student. I am grateful to Prof. Jeremy Klosterman for giving me the opportunity to be his TA for CHEM43A course. I would also like to thank my students- especially those who followed me to my other discussion sessions. I enjoyed teaching all of you. I hope that I made organic chemistry lab a little more enjoyable and interesting than you thought it would be.

I want to thank Amy and Jeff in the Chemistry office for always being there to help, not only with TA assignments but also any other issues that came up. Being an international student,

it was a tough transition which was made easier by these very warm, welcoming and amazing people at the Chem department. I would not have reached this stage of writing and defending my thesis if it wasn't for my friends and peers. Connie, Christian, Meihan, Hema, Chris and Clark have been my pillars of support during a very tough and challenging personal year. A big thank you to my roommates and very close friends, Manas and Balaji, for taking care of me and being there for me when I could not even stand on my own. I will forever be grateful for your care and wisdom. A special mention to Swetha, Ajith, Ayush, Pranav and Anantha for never giving up on me and making sure that I got back up on my feet (both literally and figuratively). Also, a big thank you to Vivek, Suyash, Chandana, Jaya, Beni, Fadi, Kanda, Hathim, Sid, Surabhi, Thanvi and Shubhangi, who made sure that I knew I was loved and who have been standing by me for many years. Thank you to all these people, my family away from family, for coming into my life at different stages and making your presence felt. If it wasn't for your support, I would not have completed my thesis. Lastly, thank you Shradha for your help with formatting and sitting with me on all those nights working on the slides and proofreading my thesis. Thank you for your positivity.

Lastly, I would like to thank my family for all their love and support. Although I mention my immediate family in the dedication, this thesis is really dedicated to my whole family- extended family back home in India and friends who became my family here away from home. There are too many people to list and I did not want to forget anyone. They are a big part of my life and they always made time for me.

ABSTRACT OF THE THESIS

Computational Prediction and Site-directed Mutagenesis Studies

of Small Molecule Binding to Fascin

by

Aashish Shivkumar

Master of Science in Chemistry

University of California San Diego, 2019

Professor Jerry Yang, Chair

Alzheimer's Disease is the most prevalent and devastating age-related neurodegenerative disease. Symptoms such as decline in memory and learning typically precede neuronal loss. The small molecules BTA-$EG_{4/6}$ have been shown to promote memory and learning, a phenomenon attributed to increased dendritic spine density. The mechanism behind this phenomenon, however, is not well understood. The work in this thesis is motivated by this gap in knowledge.

Previous studies in the Yang lab have identified Fascin as a cellular target of BTA-EG_4. Chapters 1 & 2 provide a summary of Alzheimer's disease, the spinogenic molecule BTA-EG_4 and the structure and function of fascin. In chapter 3, an *in silico* model of the binding mode of

BTA-EG_6, an analog of BTA-EG_4, to fascin is reported. In chapter 4, site-directed mutagenesis studies and other biochemical assays to characterize the residues involved in the binding site of fascin-BTA-EG_6 complex are presented. Results from circular dichroism spectroscopy and slow sedimentation actin bundling assay showed that fascin and fascin mutant proteins were functional and properly folded. Isothermal titration calorimetry results (ITC) confirmed the physical binding between fascin and BTA-EG_6 in the micromolar range. ITC data for mutant proteins revealed that mutation in the protein affected its binding affinity with BTA-EG_6. The data obtained points towards a possible mechanism of binding between BTA-EG_6 and fascin. The *in silico* model together with the biochemical data supports the participation of residues Ala137, Gly393, Ile45 and Arg389 in the binding mode of BTA-EG_6 to fascin.

Chapter 1

Introduction: Alzheimer's Disease and its Therapies; Spinogenic Molecules

1.1 Alzheimer's Disease

Alzheimer's Disease (AD) is the most prevalent age-related neurodegenerative disease and the most common form of dementia[1]. Symptoms such as decline in memory and learning typically precede neuronal loss. Eventually, it is difficult for the person to perform even basic tasks like walking and swallowing. People in the latter stages of the disease are bed-ridden and require intensive care. AD is ultimately fatal as people succumb to acute complications of the disease such as pneumonia and heart failure[4]. It is the sixth leading cause of death in the United States[5].

The greatest risk factor for the onset of AD is age. It is estimated that around 5.7 million Americans of all ages live with Alzheimer's Disease, of which approximately 5.5 million people are of age 65 and older. The frequency of AD in the general population is expected to increase together with the increase in life expectancy of the general population. It is projected that the number of AD patients in America will nearly triple and the cost of care would cross one trillion dollars by 2050[1].

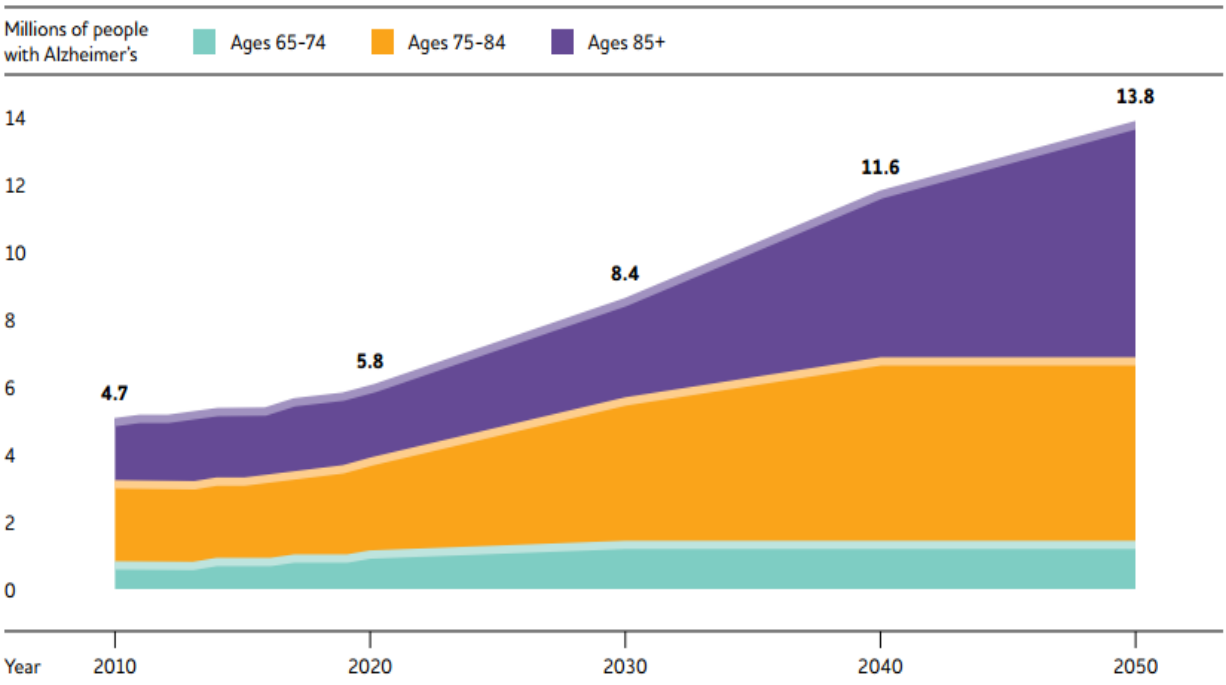

Figure 1.1: Projected number of people age 65 and older (total and by age) in the U.S. population with AD, 2010 to 2050[1].

The impacts of AD are clearly far-reaching. Its effects can be seen on the small scale of individuals as well as on a much larger scale with the government and the economy. Despite these efforts, there is no cure for AD yet. This motivates the research to understand the disease. It is crucial to find methods or develop therapeutics to ideally reverse or minimally slow the progression of AD.

1.2 Therapeutic Strategies for Treatment of AD

Although there is no cure for AD currently, there are 5 drugs that have been approved by the FDA to combat the symptoms of AD. These drugs target the imbalance of neurotransmitters–acetylcholine and glutamate.

It has been shown pharmacologically that acetylcholine (ACh) is critical for learning and for the formation of new memories[6]. A potential therapeutic strategy against AD could be to

increase the levels of acetylcholine in synapses. One way of promoting cholinergic function[7] is to inhibit the enzyme Acetylcholinesterase (AChE), which catalyzes the hydrolysis of acetylcholine[8]. Examples of FDA approved acetylcholinesterase inhibitors include galantamine[9], rivastigmine[10] and donepezil[11]. Glutamate plays a major role in normal brain function and development[12]. Abnormalities in the glutamate-glutamine cycling[12] or glutamate reuptake have been linked with synaptic pathology and neurodegeneration[13]. NMDA receptor antagonists have been developed to combat this pathology[14]. Memantine is the only FDA approved NMDA receptor antagonist on the market[15].

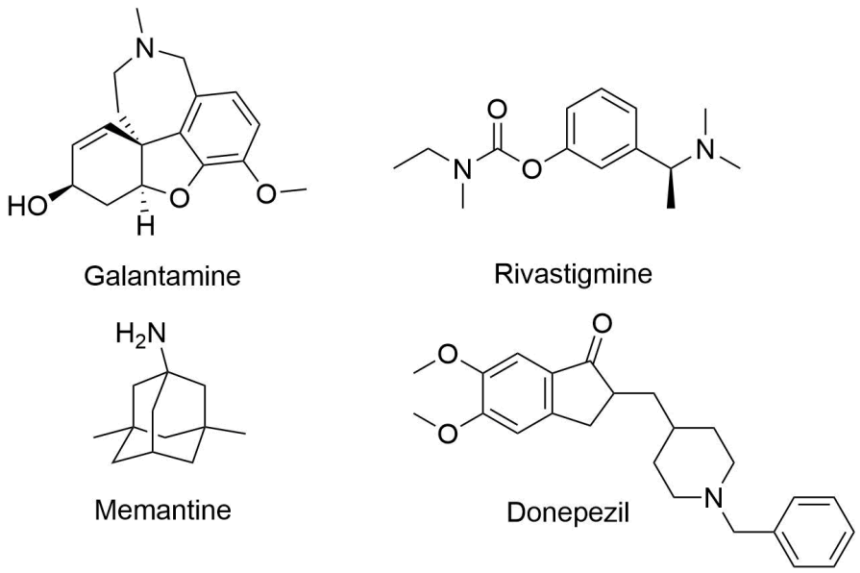

Figure 1.2: Chemical structures of current FDA approved AD drugs.

Though both classes of drugs work in different ways and do not intervene in AD pathology, these drugs may help manage and mitigate some of the symptoms of AD[16]. In addition, evidence with respect to the effectiveness of these drugs has received mixed reviews[15,17]. Hence, new drugs and therapies are needed to combat AD and other related forms of dementia.

1.3 Amyloid Cascade Hypothesis

Even though the exact cause of AD is not completely understood, there are many pathologies that have been developed that define the disease and give clues about the cause. It has been over 100 years since Alois Alzheimer noted the presence of abnormal fibrous inclusions[18] and pointed out that AD could have a distinct and recognizable neuropathological substrate[19]. The two hallmark pathologies associated with AD revolve around accumulation of extracellular senile plaque deposits of β-amyloid peptide (Aβ) and the flame shaped neurofibrillary tangles of phosphorylated tau protein[20].

Deposits of Aβ peptides have been widely seen in the post-mortem of brains of patients with AD[19]. β-amyloid is a small peptide that is derived from a larger membrane bound protein called Amyloid Precursor Protein (APP)[21]. In its activated state, APP extends from inside brain cells to outside by inserting into membranes[21]. Sequential proteolytic cleavage of APP by two membrane bound endo-proteases, β and γ-secretases, results in the formation of numerous different Aβ-peptide species[20](Figure 1.3). The most abundant isoforms of Aβ are the 40($A\beta_{1-40}$) and 42($A\beta_{1-42}$) residue peptides which can form oligomeric assemblies that purportedly lead to plaque depositions. The major isoform of Aβ deposited in senile plaques are the longer peptides (Aβ 42) which are more hydrophobic[20] and fibrillogenic in nature and have been shown to aggregate faster[18]. According to the amyloid cascade hypothesis, these stages of β-amyloid aggregation disrupt cell-to-cell communication, activate immune cells and trigger inflammation ultimately causing the destruction of brain cells[21].

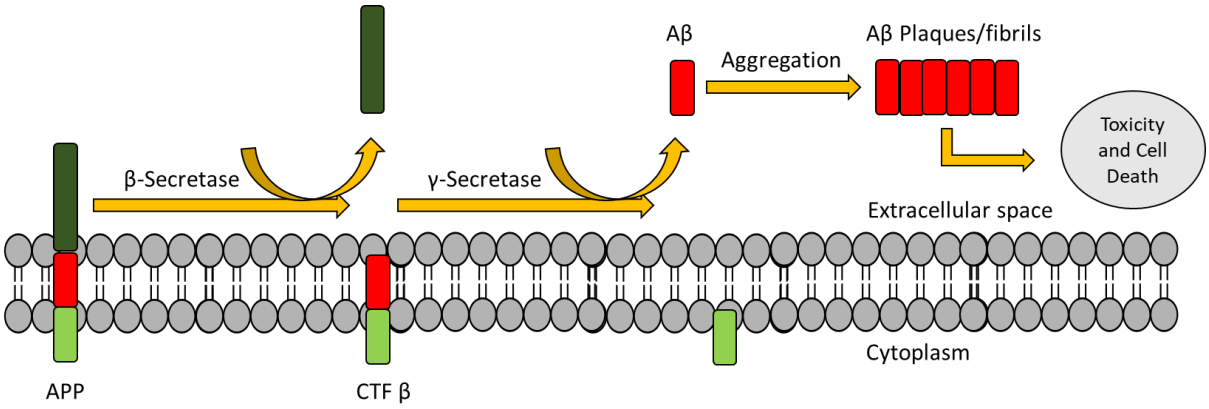

Figure 1.3: The amyloid cascade hypothesis. APP can be cleaved by β-secretase and subsequently by γ-secretase to yield Aβ. Aβ can aggregate into plaques which are toxic and cause cell death.

Though β-amyloid is produced as a non-toxic soluble metabolic product of APP, it is evident from experimental cell culture and *in vivo* data that aggregated Aβ is toxic to neurons[22]. However, the precise reason and the peptide form responsible for neurotoxicity is unclear. One hypothesis is that plaques play a role in increasing oxidative stress for cells[23]. A marked imbalance between the reactive oxygen species (ROS) and its removal by antioxidant system causes oxidative stress[24]. The net effect of oxygen radicals is damage to proteins and DNA, and this damage can cause cell death.

1.4 Targeting Amyloid Plaques as a Therapeutic Strategy

There are various potential targets to prevent AD progression and pathogenesis that include inhibiting the β-amyloid formation or increasing its clearance from the brain or inhibiting the oxidative stress induced by β-amyloid peptide[25] (Figure 1.4).

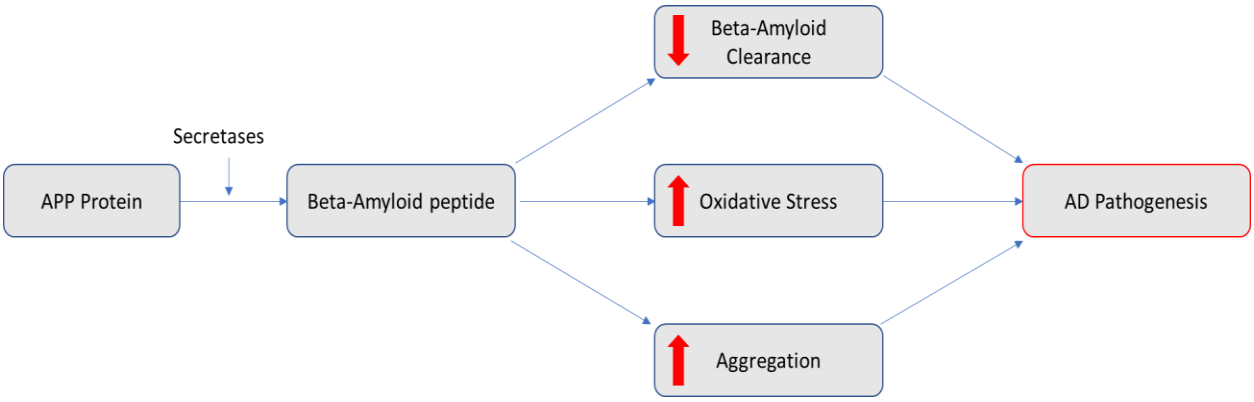

Figure 1.4: Potential therapeutic targets for AD.

Current FDA approved drugs only provide relief of symptoms to a subset of AD patients. Clearly, there is a need to explore for novel AD therapeutics to intervene, slow the disease further, halt or even reverse the neuropathic effects associated with AD and related diseases.

Over a span of 10 years, the Yang lab has developed small molecules that target amyloid aggregates. The rationale behind this strategy is that Aβ toxicity could be caused due to interaction between essential cellular proteins and aggregated Aβ peptides. In particular, the Yang lab has investigated the interference of Aβ with the proteins responsible for regulating reactive oxidative species levels in the cell[26,27]. Disrupting these interactions may lead to reduced Aβ toxicity.

Small molecules such as Congo Red (CR) and Thioflavin-T (ThT) have been historically used to stain and visualize amyloid plaques[28]. Experiments carried out in the Yang lab demonstrated that it is possible to partially inhibit the interaction of anti-Aβ Immunoglobulins (IgG) raised against Aβ with soluble fibrils formed from synthetic Aβ peptides by using staining agents like ThT[29]. But since CR and ThT are charged molecules, it limits their application *in vivo*. In subsequent studies, the Yang group designed and synthesized new uncharged derivatives of Thioflavin-T. Structural modifications by incorporation of an oligoethylene glycol chain and

removal of the charged N-methyl group were designed to improve the biocompatibility yet retain the water solubility properties of the new derivatives[27] (BTA-EG_4 and BTA-EG_6) (Figure 1.5).

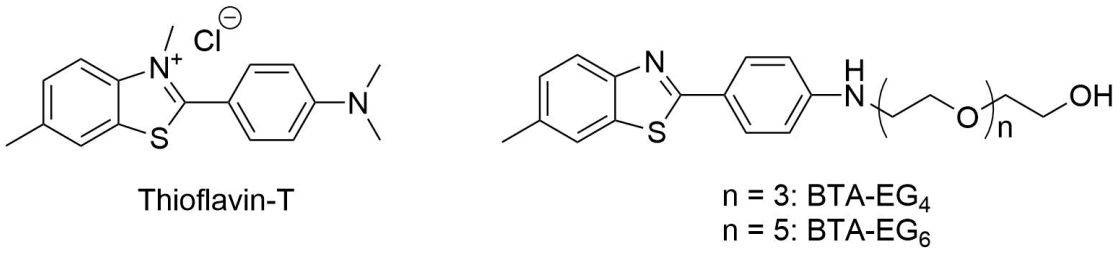

Figure 1.5: Chemical structures of amyloid-binding small molecules.

On examination, these two oligo (ethylene glycol) derivatives of ThT inhibited the IgG-fibril interaction more effectively than ThT[27]. In addition, due to increased cell membrane permeability, both the derivatives were found to be more biocompatible[30].

They also investigated the contribution of protein-amyloid interaction towards Aβ induced oxidative stress. The effect of BTA-$EG_{4/6}$ molecules on SH-SY5Y neuroblastoma cells treated with aggregated Aβ demonstrated that BTA-$EG_{4/6}$ molecules could rescue those cells from some toxicity associated with Aβ. This observation was attributed to the ability of BTA-$EG_{4/6}$ to interfere with catalase-amyloid interactions, which inhibit catalase and increase oxidative stress in the cell[26].

1.5 BTA-$EG_{4/6}$ - Spinogenic Molecules

Benzothiazole aniline (BTA) family of compounds are a class of small molecules that have shown great promise in decreasing Aβ induced toxicity in the cell by interfering with the interaction between aggregated Aβ and associated proteins such as catalase[26]. Investigation of biological effects of BTA-$EG_{4/6}$ *in vitro* and *in vivo* showed that BTA-$EG_{4/6}$ appeared to improve memory and learning in an AD mouse model[31,32]. This observation was attributed to increased dendritic spine density in neurons, a phenomenon known as spinogenesis. Surprisingly, these

effects were also seen in wild type mice that do not express human forms of Aβ[31,32].These results suggested that the observed phenotype induced by BTA-$EG_{4/6}$ is independent of the presence of Aβ aggregates.

Dendritic spines are small actin rich protrusions that arise from the surface of dendrites[33]. Morphologically, these dendritic spines can be thin, hair-like (filopodium), stubby, mushroom and cup shaped[34]. They have a bulb-like head which is connected to the main body of the dendrite by a thin neck (Figure 1.6). Functionally, they form the postsynaptic part of excitatory neuron and receive signals from the axon of presynaptic neuron. These dendritic spines are very important sites for communicating information and for processing and storage in the brain[35]. Consequently, AMPA receptors and NMDA receptors can also be found on the surface of dendritic spines[36].

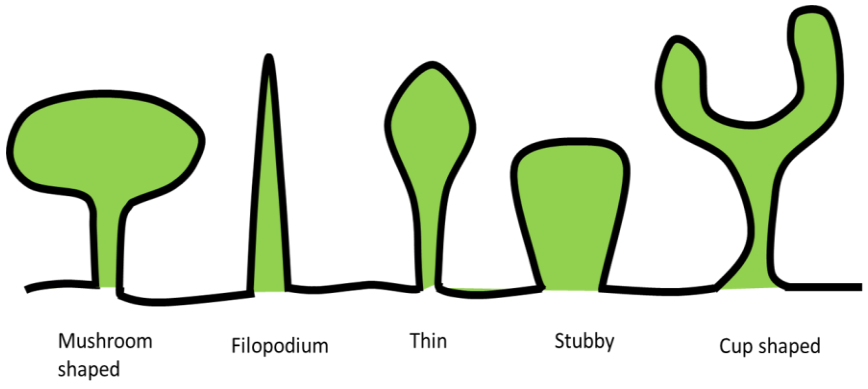

Figure 1.6: Morphological classification of dendritic spines.

Spines contain many proteins that are essential for their function, but actin[35], a cytoskeleton protein, is most abundant. Actin is useful to provide the necessary framework for maintaining the structure and architecture of the dendritic spine[35]. The presence of actin makes the dendrites very dynamic in nature, hence they can reassemble and disassemble very rapidly[34]. Experimental evidence obtained by artificial simulation of hippocampal[37] slices and training in animals[36,38,39] is

indicative of the development of dendritic spines and their role in the acquisition of new memories and learning[40,41].

Alteration or decrease in dendritic spine density is another pathology seen in AD[42] and other neurological disorders like autism spectrum disorder (ASD) and schizophrenia[43]. Since the existing evidence strongly points towards a relationship between dendritic spines and memory, an effective therapeutic strategy to combat AD and other neuropathic disorders would be to modulate the density of dendritic spines. Apart from the phenotypic ability of BTAEG$_{4/6}$ to induce spinogenesis, a lot remains unclear about the mechanism of action of these intriguing molecules.

1.6 Cellular Target of BTA-EG$_{4/6}$

Dr. Kevin Sibucao, a former Ph.D. student in the Yang lab, employed a photoaffinity labeling approach to identify the cellular binding partners of BTA-EG$_4$. The BTA-EG$_4$ based probe contained a trifluoromethyl diazirine for crosslinking and biotin for subsequent affinity pulldowns. Photoaffinity labeling and competition assay in cell lysates of human cortex successfully identified that BTA-EG$_4$ targets a 55-kDa protein. Next, affinity pull down experiments using neutravidin-agarose resin were performed in SH-SY5Y neuroblastoma cells to isolate the 55 kDa protein. Tandem mass spectrometry determined the most prominent protein as Fascin 1 (here on referred as fascin). Subsequent western blot analysis using a fascin antibody verified the presence of fascin. In addition, pulldown studies with human cortex and mouse midbrain tissue demonstrated that the results observed in SH-SY5Y cells translated to different tissue types.

The interesting activities shown by BTA class of molecules and the unknown details behind the mechanism of BTA-EG$_{4/6}$ induced spinogenesis motivate the work in this thesis. In this thesis, I will focus on fascin. In chapter 2, I provide a brief survey of this protein. To gain mechanistic

insight into BTA induced spinogenesis, I characterize the protein-ligand interaction between fascin and a BTA-EG_4 analog, BTA-EG_6, in order to develop a better quantitative understanding of how BTA-EG_6 interacts with fascin. In Chapter 3, I propose a computational model for the binding mode of fascin-BTA-EG_6 complex. In Chapter 4, I report biochemical experimental results that provide clues to validate the proposed computational model.

Chapter 2

Fascin as Target for BTA-EG4/6

2.1 Structure and Function

Fascin refers to a class of proteins that bind and bundle filamentous actin (Figure 2.1). Fascin was first discovered by Robert Kane in the 1970s during a procedure to isolate filamentous actin (F-actin) from sea urchin egg extracts[44]. He observed that these extracts formed a gel that contained two other cytoplasmic proteins (approximately 58 kDa and 220 kDa) in abundance along with actin[45]. Ultimately, the 58 kDa protein was named "fascin" due to its ability to group F-actin into filopodial cores and cross- linking actin filaments into fascicles[46].

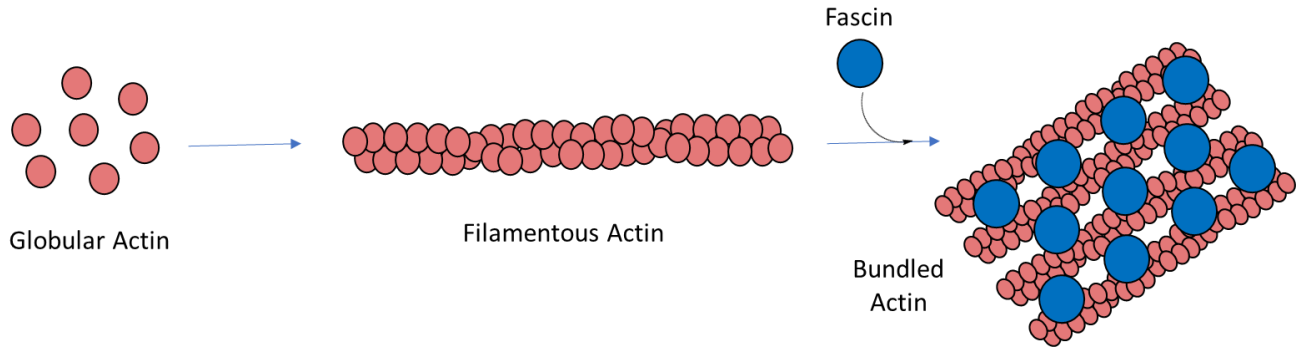

Figure 2.1: Globular actin polymerizes into actin filaments and these filaments are grouped together by fascin.

After the discovery of fascin, other proteins exhibiting similar activity were found. In 1985, Yamashiro-Matsumura *et al.* found that gelation of F-actin could be induced from soluble extracts of HeLa cells. They were able to isolate a 55 kDa protein from the gel[47]. A few years later, in 1993, Bryan *et al. c*loned and expressed the cDNA sequence for an echinoid actin bundling protein[48]. The peptide sequence of this protein and the sequence of Yamashiro-Matsumura's 55 kDa protein showed high levels of similarity[48]. Owing to all these observations, these proteins were grouped

together as “fascin” proteins[48]. Homologs of fascin are also found in other organisms such as mouse[49] and xenopus[50].

There are three isoforms of fascin found in mammals, each labeled 1, 2 and 3 respectively. Fascin 1 is found in many tissue types and in different quantities. For example, fascin 1 is found in high abundance in the brain and very low quantities in the small intestine and spleen[49]. On the other hand, fascin 2 and 3 are restricted to only one tissue type. Fascin 2 is expressed in the retina while fascin 3 is expressed in the testes[51].

Fascin is a globular, monomeric protein that has structurally been found to bind actin in a 1:4 stoichiometry[52]. Extensive research on fascin has resulted in multiple crystal structures of fascin over the past two decades[2]. The crystal structure found by Sedeh *et al.* revealed a novel arrangement of 4 tandem β-trefoil domains. These are grouped into two pairs and act semi independently from each other.

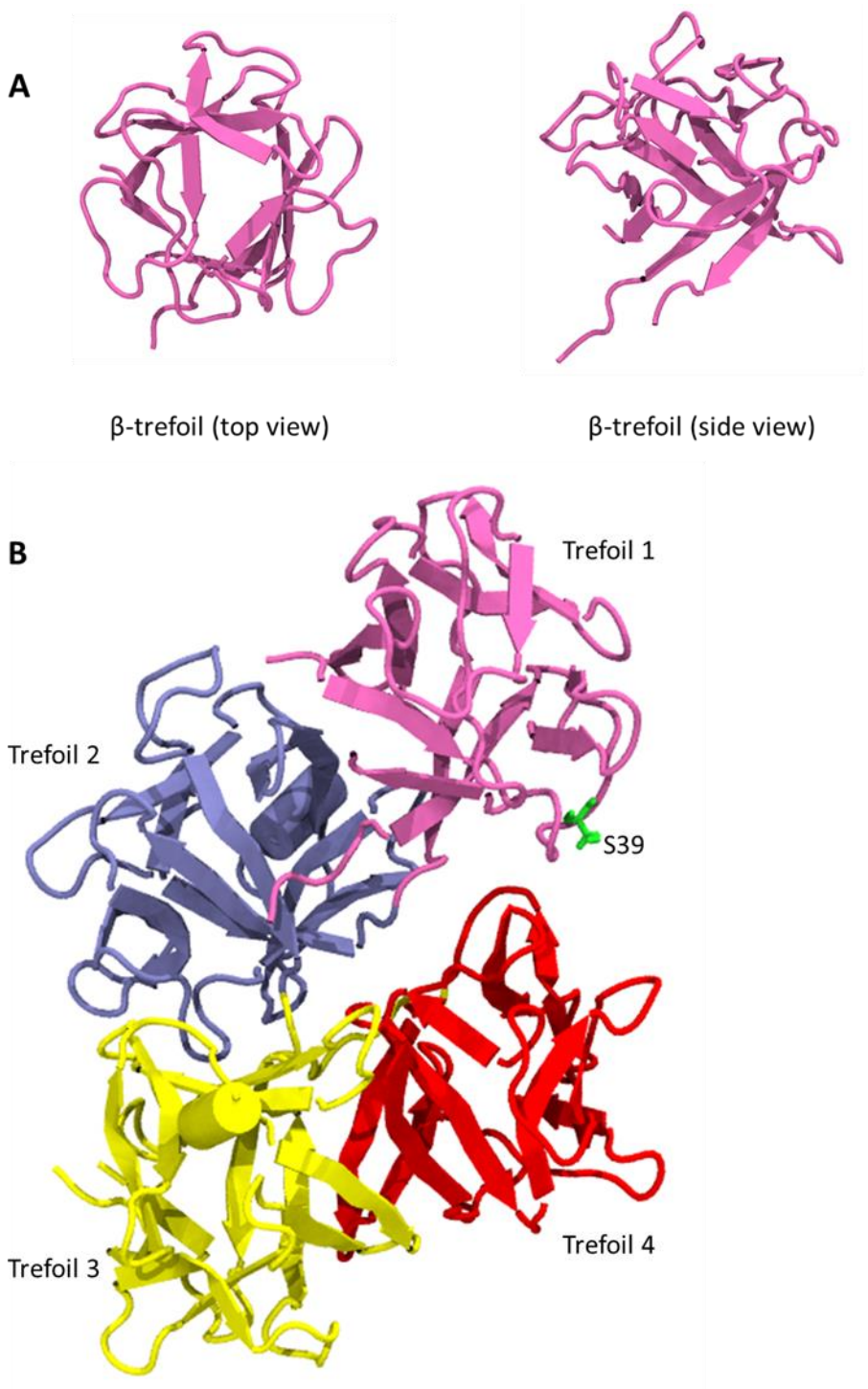

Figure 2.2: (A) Trefoil 1 as a representation of a β-trefoil[2]. Top view exhibits a barrel like structure formed by the β-sheets. (B) Crystal structure of fascin[2] (PDB ID:1DFC) with the regulatory site Ser39. Fascin comprises of two domains which are related by a pseudo 2-fold symmetry.

Ono *et al.* found a regulatory site on fascin. They found that fascin's ability to bind and thus bundle actin is greatly diminished on phosphorylation at Ser39 by Protein Kinase C (PKC)[53]. The phosphorylation site contains several lysine residues that play a critical role in actin binding[53,54]. Upon phosphorylation, the interaction between the positively charged actin binding site and the negatively charged phosphoryl group may interfere with actin binding[53].

Jansen *et al.* elucidated some mechanistic aspects of fascin's actin bundling activity[54]. They found that domains 1 and 3 contained highly conserved sites and investigated further by making fascin mutants at these sites and determined how these mutations affected fascin's actin bundling activity. They also found that some of these mutations disrupted cells' ability to develop filopodia.

Filopodia are thin cell membrane projections that play an essential role in cellular functions such as cell migration and adhesion[55]. Regulation, polymerization and cross linking of actin filaments is needed for the development of filopodia. In other words, fascin's actin bundling activity is crucial to provide crosslinked actin bundles that are necessary for the structural support of filopodia[55]. In experiments performed with mouse melanoma B16F1 cells, RNA interference of fascin and knockdown of fascin resulted in overall reduced number of filopodia with abnormal morphology lacking bundled actin[56]. Thus, these RNAi experiments reinforce that fascin is necessary for proper filopodia formation[56].

2.2 Other Binding Partners of Fascin

2.2.1 β-catenin

β-catenin is a multitasking and evolutionarily conserved protein. It participates in the Wnt signaling pathway which is involved in regulating cellular proliferation, differentiation and homeostasis[57]. In addition to its role in Wnt pathway, β-catenin forms an integral structural

component of the cadherin complex by binding to an ensemble of cadherins[58]. Cadherins are transmembrane proteins that mediate adhesion by interacting with other cadherin proteins on other cells[59]. Newly synthesized β-catenin associates with the intracellular portion of cadherin, gets immobilized by E-cadherin specifically and, in coordination with α-catenin, interacts with the actin network thereby indirectly modulating the actin cytoskeleton[59]. Further, Tao *et al*. found that β-catenin binds directly to fascin. They demonstrated the association of β-catenin with fascin by carrying out a yeast two-hybrid screen and immunoprecipitation experiment[60]. While the function of this β-catenin-fascin complex has not been well characterized, it was observed that the complex colocalizes at the leading edge of cells[60].

2.2.2 LIM Kinase 1

LIM kinase (LIMK) 1 and 2 comprise the LIM kinase family of proteins which is the downstream target of Rho GTPases signaling pathway[61]. The Rho signaling pathway can be conceptualized as a relay of messengers (Figure 2.3). Cells receive extracellular stimuli that trigger guanine-nucleotide-exchange factors (GEFs) and GTPase activating proteins (GAPs) to activate small GTPases like Rho. In turn, Rho activates its downstream effectors, which send the signal to another downstream protein and so on until the signal reaches its destination[62]. Rho kinase I and II (also known as ROCK1 and ROCK2) are key Rho effectors that activate LIMK1 by phosphorylating it. LIMK1 is known to regulate actin dynamics and the architecture of the actin cytoskeleton within the cell. One of its downstream targets is the actin-severing cofilin family of proteins[63].

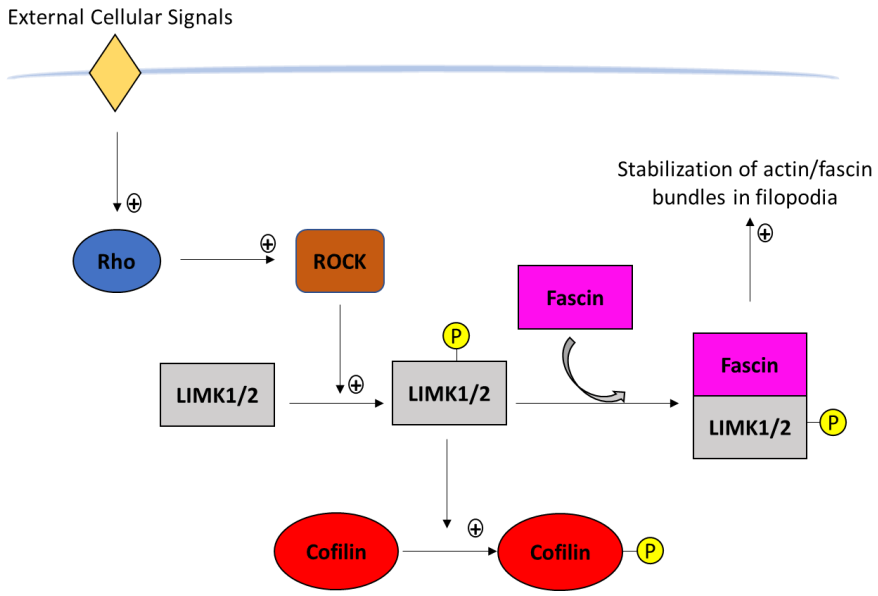

Figure 2.3: Rho signaling pathway, LIMK1 and Fascin.

In 2012, Jayo *et al.* discovered that LIMK1 binds to fascin[64]. It was observed that binding between fascin and actin was disturbed upon inhibition of either Rho or its effectors by endotoxin C3[64]. The authors performed Fluorescence Resonance Energy Transfer (FRET) and affinity pull-down studies in skeletal myoblasts and human colon carcinoma cells to specify the part of the Rho signaling pathway that was targeted. The results showed that there was direct interaction between LIMK1, as well as LIMK2, and fascin. Subsequent *in vitro* experiments revealed that the LIMK1-fascin interaction regulated filopodia stability[64].

2.2.3 L-Plastin

Plastins are a family of highly conserved actin-binding proteins[65]. Two plastin isoforms, T and L, have been identified in humans. T-plastin has been found in solid tissues like endothelial and epithelial cells while L- plastin is only expressed in hemopoietic cell lineages[65]. Conversely, *in vivo* and *in vitro* experiments have shown that aberrant L-plastin expression enhances proliferation, invasiveness and lethality of tumor cells[66]. Due to this activity, L-plastin is

considered as a common marker of many cancer types. Audenhove *et al.* identified L-plastin's role in degradation and invasiveness of cancer cell filopodia and invadopodia[67]. Their experimental results established a cooperative mode of action between L-plastin and fascin. L-plastin differs from fascin and forms thinner and loosely packed actin bundles. Their results show that composite bundles formed by L-plastin and fascin together adopt an intermediate structural phenotype, with plastin accounting for flexibility that is essential for elongation and fascin providing strength for protrusive force and stability[67].

2.2.4 Rab35

Rab35 is a member of the Rab family of proteins which makes up the largest subset of the Ras super family of small guanosine triphosphatases (GTPases). Rab proteins are evolutionarily conserved and regulate membrane transport processes[68]. Members of the Ras superfamily share some common biochemical properties. They bind to GTP and can hydrolyze their bound GTP into GDP[69]. Regulation of the activity of these proteins depends on the phosphorylation state of the bound guanosine nucleotide (Figure 2.4). The protein is in active state conformation when it is bound to GTP and is considered to be in an inactive state conformation when it is bound to GDP[69]. This GDP-GTP cycle is highly regulated by GTPase activating proteins (GAPs) and guanine exchange factors (GEFs).

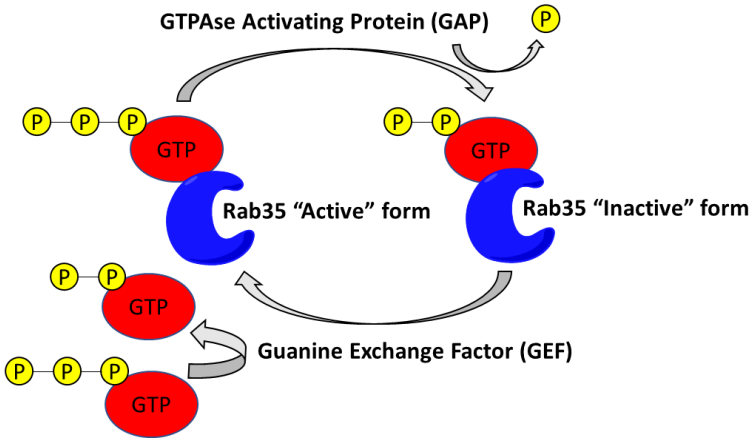

Figure 2.4: Rab35 and its GTPase activity.

Active Rab35 affects the localization of fascin to the cell membrane thus playing an important role in actin bundling[3]. Zhang *et al.* demonstrated that cells expressing a dominant negative Rab35 mutant produced less fascin at the cell membrane[3]. Furthermore, experiments performed by Chavellier *et al.* showed that Rab35 influences cell shape in an actin dependent manner[3,70]. They observed an increase in neurite growth in N1E-115 neuroblastoma cells that expressed constitutively active Rab35 mutant while decreased growth was seen in Rab35 silenced cell lines[70].

2.3 Fascin in Neurons

In neurons, fascin is found abundantly in growth cones[71]. Neuronal growth cones are motile structures present on the elongating tip of the nerve axons. These structures guide the axon to reach its target[71] and are critical for the development of the nervous system as they can sense chemotropic cues[72]. Fascin is involved in developing filopodia which are essential for growth cone motility[72]. Since filopodia and dendritic spines are both cell protrusions, fascin would be expected to be involved in dendritic spines as well. Surprisingly though, filopodia are fascin positive and dendritic spines are fascin negative[73]. Korobova *et al.* demonstrated distinguishable structural characteristics

of dendrites and filopodia[73]. Filopodia contain tightly bound parallel bundles of actin filaments while dendritic spines contain branched and shorter actin filaments[73]. In some cases, loosely bound long actin filaments are also found in the neck of a dendritic spine[73]. These structural differences may be attributed to the different actin binding proteins in each structure. Dendritic spines contain a protein complex called the Arp2/3 which is responsible for actin branching[73]. This protein complex in absent in filopodia. Such observations are important to understand the mechanism and the role of BTA-$EG_{4/6}$ molecules in inducing spinogenesis.

2.4 Implications in Disease

Fascin is absent in most normal epithelia but is found in metastatic cancers. Tan *et al.*, by carrying out a systematic review and meta-analysis of various immunohistochemical studies, demonstrated that fascin is linked consistently with increased risk of mortality and metastasis in breast, colorectal and gastric cancers[74]. Fascin serves as a biomarker for identification and early diagnosis of potentially aggressive cancers.

A common feature of all metastatic cancers is the ability of cancer cells to move and invade surrounding healthy tissues[75]. Fascin is used by the cells to make long filopodia-like actin based degradative protrusions called invadopodia[87]. These allow cancer cells to migrate by breaking down the extracellular matrix[76]. Studies observed that fewer, shorter and less persistent invadopodia were formed as a result of fascin knockdown[77], thus elucidating its role in the formation of invadopodia. Due to its involvement in cell motility, fascin can be targeted as a potential therapeutic which can be exploited to halt or destroy the metastasis of cancer.

2.5 Implications on Drug discovery

Fascin has been the focus of much drug discovery work owing to its involvement in metastatic cancer. Migrastatin, a novel antibiotic with a unique 14-membered macro lactone ring, has been shown to inhibit cell migration of human esophageal cancer EC17 cells and mouse melanoma B16 cells[78]. In consequent studies, Migrastatin analogues have been shown to be potent inhibitors of cell migration and invasion of metastatic tumors[79]. One of the analogues, macroketone, interestingly targets fascin and is able to inhibit its actin-bundling activity[79].

Compounds that target fascin have also been identified in chemical libraries[80]. Following up the work done with Migrastatin and macroketone, Huang and coworkers investigated a library of around 165,000 compounds to find small molecule inhibitors of fascin's actin bundling property[81]. They developed a high-throughput imaging-based screening assay to visualize the effect of small molecules on actin bundling and discovered 15 compounds that inhibited fascin's bundling activity[80]. In particular, extensive work was done on G2 which demonstrated the ability to stop cancer migration[80]. The authors also generated fascin mutants to investigate the actin bundling site and assess the mutant's ability to bundle actin. Mechanistically, their studies indicated that G2 binds to an actin binding site on fascin[80].

A cell-based bioassay was developed by Kraft *et al.* to screen small molecules that target fascin-related biological pathway modulators[82]. Although none of these small molecules have been confirmed to bind directly to fascin, they appear to modulate a fascin-dependent phenotype in the morphology of Drosophila neurons. They were able to take advantage of the "filigree" phenotype seen in cultured Drosophila neurons with a mutated *singed* gene[82] (considered as Drosophila version of fascin). The *singed* mutation causes striking disruptions in actin cytoskeleton. The neurons with such a mutation develop curved offshoots that are distinguishable from normal

neurons. It is noteworthy that the screening library contains not only fascin pathway blockers that have anti-metastasis potential but also enhancers with cognition-enhancing abilities, some of which are already FDA approved drugs[82].

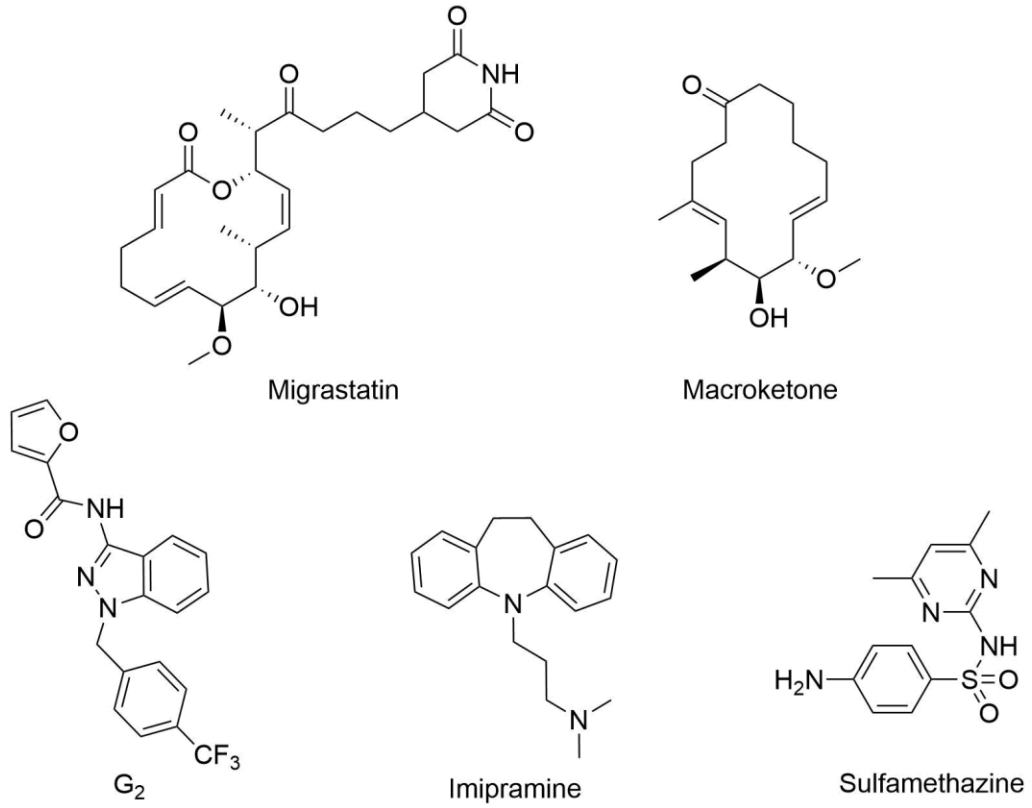

Figure 2.5: Chemical structures of Migrastatin, Macroketone, G2, Imipramine (fascin pathway blocker) and Sulfamethazine (fascin pathway enhancer).

2.6 BTA-EG4/6 Induced Spinogenesis

Little has been reported in literature about fascin's role in dendritic spines and spinogenesis however, it is found in abundance in filopodia. This lack of literature data may suggest that fascin is not directly involved in forming dendritic spines. By extension, BTA-EG4/6 also should not directly affect this process. Using all these conclusions, Dr. Kevin Sibucao in the Yang lab focused on the idea that dendritic spines are distinct from filopodia in order to develop a hypothesis for

BTA-$EG_{4/6}$ induced spinogenesis (Figure 2.6). He proposed that the relative abundance of actin is in equilibrium and can be destined to be part of a filopodium or a dendritic spine. Pulldown assays revealed that BTA-EG_4 inhibited the interaction between fascin and Rab35. Inhibition of this interaction may prevent fascin's recruitment to the cell membrane. With less fascin available at the cell membrane, the development of filopodia will be hindered[3]. A consequence of this phenomenon would mean availability of more actin that can be dedicated towards dendritic spine formation and thus result in increased spine density.

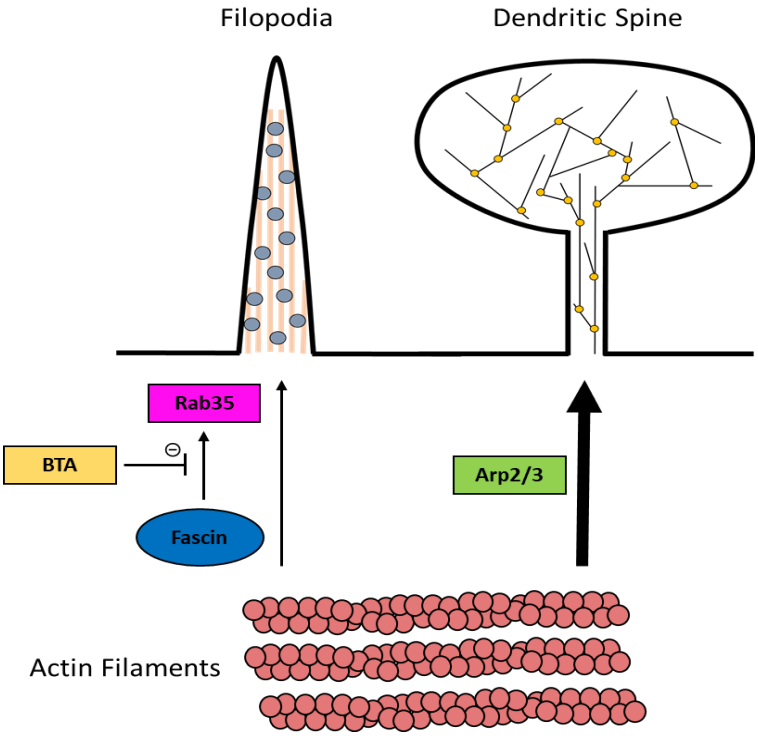

Figure 2.6: Model for BTA-$EG_{4/6}$ induced spinogenesis. Actin could be used to build filopodia or dendritic spines. Inhibition of Rab35[3] and fascin interaction by BTA-$EG_{4/6}$ may hinder filopodia formation, leading to an increase in the pool of actin and promoting the formation of dendritic spines.

Previous experiments have demonstrated that BTA-EG_6, an analog of BTA-EG_4, exhibits similar spinogenic properties[32]. It was noted that the use of BTA-EG_4 in biochemical experiments was limited due to its poor solubility in water, whereas the two extra ethylene glycol units in BTA-

EG_6 molecule dramatically increased the solubility of the compound. Hence, I used BTA-EG_6 in all of my experiments reported in this thesis. The rest of the thesis will focus on characterizing the interaction between fascin/fascin mutants and BTA-EG_6.

Chapter 3

In silico Modeling of Fascin-BTA-EG_6 Interactions

3.1 Introduction

The application of computer-aided methods for predicting ligand-protein interactions and complexes has become increasingly useful for drug discovery[83]. Molecular docking has helped bridge the gaps in our knowledge of characterizing the behavior of small molecules in the binding site of target proteins. Molecular docking software are frequently used in the drug development area to model and study biochemical pathways. The molecular docking process, in general, can be cut down to two steps: predicting the pose of the ligand and the assessment of binding affinity[84]. The pose refers to the conformation as well as the position and orientation that the ligand takes within the binding site. Knowing the binding site before docking increases the docking efficiency.

In collaboration with Zied Gaieb and Conor Parks in the Amaro lab at UCSD, *in silico* docking experiments were performed to identify the most favorable binding mode of BTA-EG_6 ligand and fascin protein.

3.2 Molecular Docking

Based on the X-ray crystal structure of fascin, Huang and coworkers determined two actin binding sites on fascin which are essential for the formation of filopodia. One site was identified between β trefoils 1-2 and the other site was found to be between β trefoils 1-4. Multiple studies report that small molecules bind to these sites and affect fascin's functionality[52,54,80,85]. Fascin also has a regulatory site Ser39 in β trefoil 1[53]. Of the two actin binding sites on fascin,[54,85] the site between β trefoils 1-4, containing the regulatory site (Ser39), was chosen for molecular docking studies.

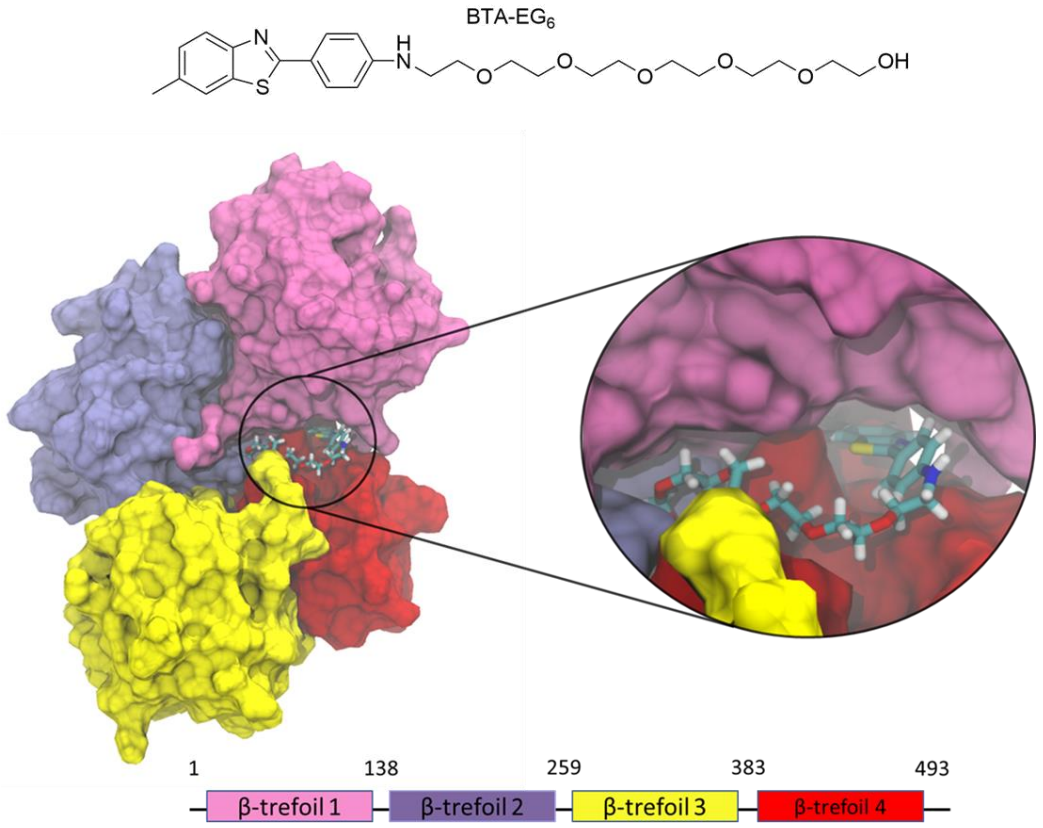

Figure 3.1: Proposed binding mode for BTA-EG_6 and Fascin (Docked to 1DFC).

In this complex, the terminal-fused benzothiazole moiety of BTA-EG_6 is surrounded by a number of hydrophobic residues including Ala137, Ile45, Leu40, Phe394 while the central benzene group is flanked by hydrophilic residues including Glu391, Arg389, Tyr458 (Figure 3.2). Both the benzene rings in BTA-EG_6 are in close proximity to form pi-pi stacking interactions with residues Tyr458, His392, His65 and Phe394 (Figure 3.2). The ethylene glycol moiety displays flexibility and samples several different conformations. In this representation, the ethylene glycol tail is buried in a hydrophilic environment surrounded by Glu258 and Glu492 on one side and solvent-exposed from the other end (Figure 3.2). It is possible that following the primary conformational selection event, optimization of side chain interactions occurs.

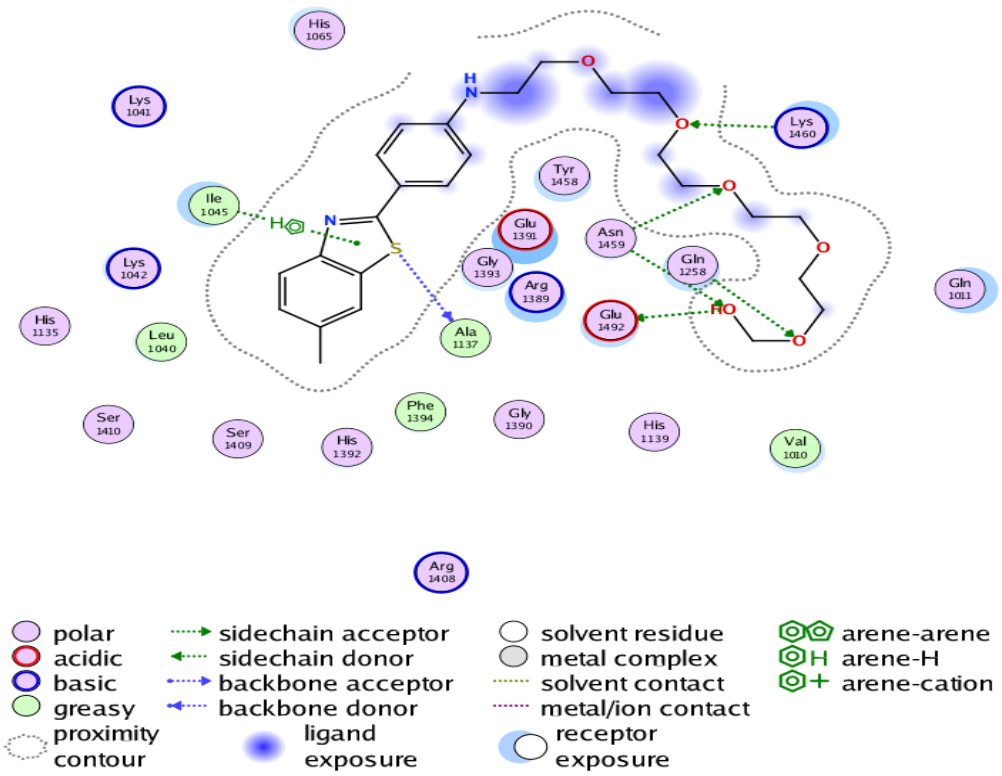

Figure 3.2: Ligand interactions in the proposed binding pocket of Fascin and BTA-EG_6.

3.3 Proposed Mutational Analysis

Next, to experimentally investigate and verify the involvement of fascin residues in interaction with BTA-EG_6, we identified specific residues to perform point mutations in the proposed binding pocket. A change in the binding affinity of the mutant fascin proteins with BTA-EG_6 can provide quantitative evidence to validate the *in silico* model. For this, we chose the residues Ala137, Gly393, Arg393 and Ile45 that form part of the binding pocket. (Figure 3.3)

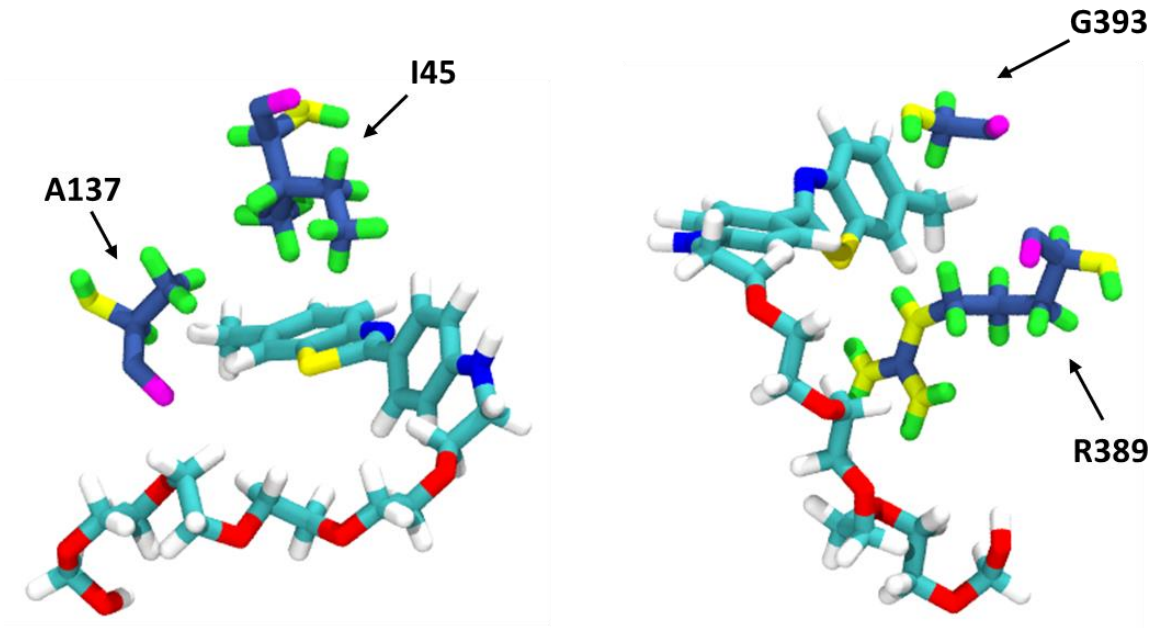

Figure 3.3: Residues in the proposed binding site chosen for point mutations- A137 and I45 are part of trefoil 1 whereas R389 and G393 comprise trefoil 4.

Ile45 and Ala137 are hydrophobic residues buried inside the cleft formed between trefoils 1 & 4. Mutating Ile45 to a polar residue such as Gln can allow for H bond interactions with Sulphur or Nitrogen atoms in the benzothiazole. Similarly, mutating Ala137 to a longer, charged species such as Lys, can induce cation-pi interaction with the benzene ring of BTA-EG_6. On the other hand, owing to its charge and large size, Arg389 is involved in multiple interactions including pi-pi interaction with the benzene ring of BTA-EG_6 and H bond interaction with the ethylene glycol tail. Mutating Arg389 to a smaller hydrophobic residue such as Ala will hamper these interactions. Gly393 is present on trefoil 4, vertically opposite to the Lys42 present on trefoil 1. Mutating Gly393 to a longer and charged residue, Glu, can give rise to a stabilizing interaction between G393E in trefoil 4 and Lys42 on trefoil 1. It can also allow for H bond interactions with the benzothiazole group of BTA-EG_6.

In the next chapter, I outline the biochemical assays to analyze the effect of these proposed mutations on the interaction between BTA-EG_6 and fascin.

Table 3.1: A list of proposed point mutations and the expected effects on binding affinity.

Residue/Position	**Mutated Residue**	**Structural Changes**	**Expected Outcome**
Isoleucine (I)/45	Glutamine (Q)	Hydrophobic to polar	Increased binding
Alanine (A)/137	Lysine (K)	Hydrophobic to charged (Longer side chain)	Increased binding
Glycine (G)/393	Glutamic acid (E)	Hydrophobic to charged (Bigger size)	Increased binding
Arginine (R)/389	Alanine (A)	Charged to hydrophobic (Smaller size-breaking existing interactions)	Less binding

Chapter 4

Characterizing Interactions between BTA-EG_6 and Fascin

4.1 Introduction

Photoaffinity labeling studies carried out by Dr. Kevin Sibucao in the Yang lab revealed that fascin is a cellular target of BTA-EG_4. *In silico* docking studies with an analog of BTA-EG_4, BTA-EG_6 were used to propose a binding mode of BTA-EG_6 to fascin. The remainder of this thesis will focus on performing site-directed mutagenesis and other biochemical assays to investigate and characterize the fascin-BTA-EG_6 interaction. The results obtained will help us to gain mechanistic insight into how BTA-EG_6 acts on fascin.

4.2 Expressing and Purifying Recombinant Wild-type and Fascin Mutant Proteins

Performing biochemical assays to investigate the fascin-BTA-EG_6 interaction requires a steady source of purified fascin. The Yang lab has previously successfully constructed a glutathione-S-transferase fascin (GST-fascin) fusion protein containing a thrombin cleavage site between GST and fascin. Briefly, recombinant GST-fascin is produced by expressing the protein in BL21 cells, followed by lysis and purification by immobilizing the fusion protein on Glutathione Sepharose 4B beads (GE). After extensive washing, the protein is eluted by incubating the bead slurry with thrombin. Thrombin cleaves the linker between GST and fascin, allowing purified fascin to elute from the beads.

Using the computational model of the proposed binding site, we came up with a set of 4 mutations - A137K, G393E, I45Q and R389A to study the binding between fascin and BTA-EG_6. The mutations were designed keeping in mind their purpose to increase or disrupt the binding affinity and hence provide quantitative evidence to verify the computational model described in

chapter 3. Site-directed mutagenesis was employed to introduce these point mutations. The same protocol for expression and purification as that of wild-type fascin mentioned above was followed.

Protein purity of recombinant wildtype and fascin mutant proteins was assessed visually by gel electrophoresis and Coomassie brilliant blue stain (Figure 4.1-A), and protein identity was confirmed by western blot (Figure 4.1-B).

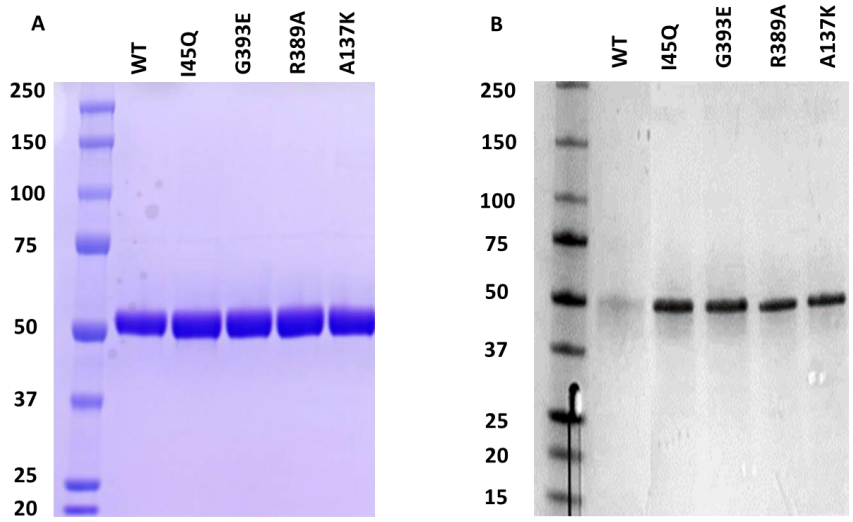

Figure 4.1: SDS-PAGE of purified wildtype and mutant fascin proteins. A) Coomassie stain of fascin after thrombin cleavage B) Western blot of fascin using an anti-fascin antibody.

4.3 Circular Dichroism

Circular Dichroism (CD) is a type of optical activity that arises due to difference in the absorption of left-handed circularly polarized light (L-CPL) and right-handed circularly polarized light (R-CPL) by a solution containing chiral molecules[86]. It is used as a tool for determining the secondary structure and folding properties of proteins that have been recombinantly expressed[87].

CD has been used in this study to assess whether the expressed, purified proteins are folded properly or if a mutation affects their conformation and stability. The CD spectra of expressed

proteins in this study were analyzed in the far UV region (wavelengths between 195-260 nm). The spectra for all the proteins show similar features expected of a structure containing β-sheets, a characteristic of the fascin molecule consisting of 4 β trefoils. The spectra for fascin mutants aligned well with that observed for wildtype thus suggesting that the mutations did not affect the proper folding of the proteins. Fascin mutant proteins, R389A and G393E, showed a shift in their spectra but results from actin bundling assay show that these are functional and hence are expected to be properly folded.

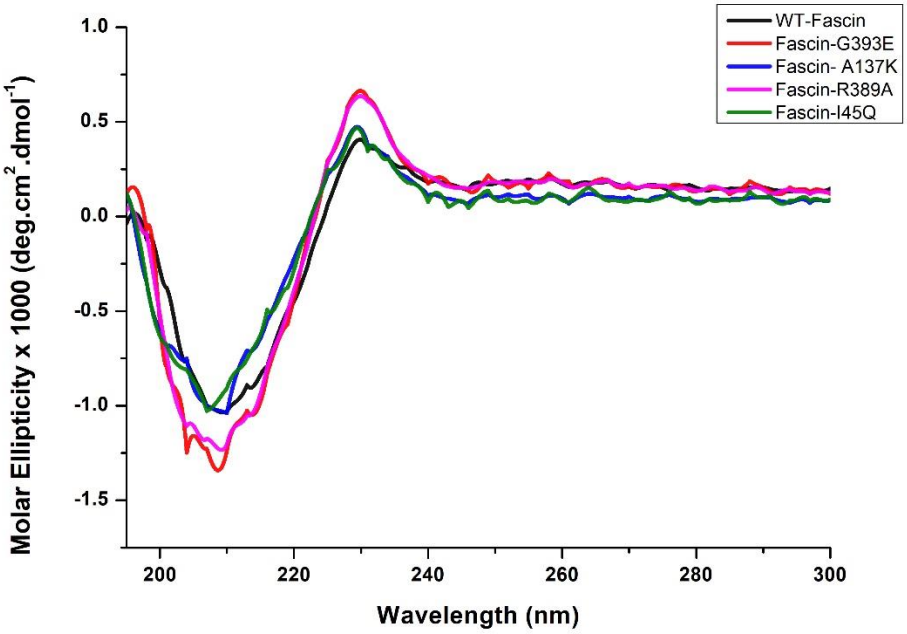

Figure 4.2: Circular dichroism spectra of *E. coli* expressed wildtype and fascin mutant proteins.

4.4 Actin Bundling Assay

To test the functionality of fascin and fascin mutants, I used an actin bundling assay[47,80] (Figure 4.3). Actin gets bundled by fascin, forming a gel-like material[45]. Upon centrifugation, the gel-like material will be pelleted out. However, unbundled actin remains in the supernatant. F-

actin was incubated in the presence and absence of recombinant fascin and fascin mutants. Most of the actin was seen in the supernatant when fascin was not present. But sedimentation of the majority of actin was observed in samples where actin and fascin were incubated together. This observation of actin sedimentation was consistent across all the fascin mutants too which demonstrates that fascin as well as fascin mutants in this study were able to bundle actin filaments.

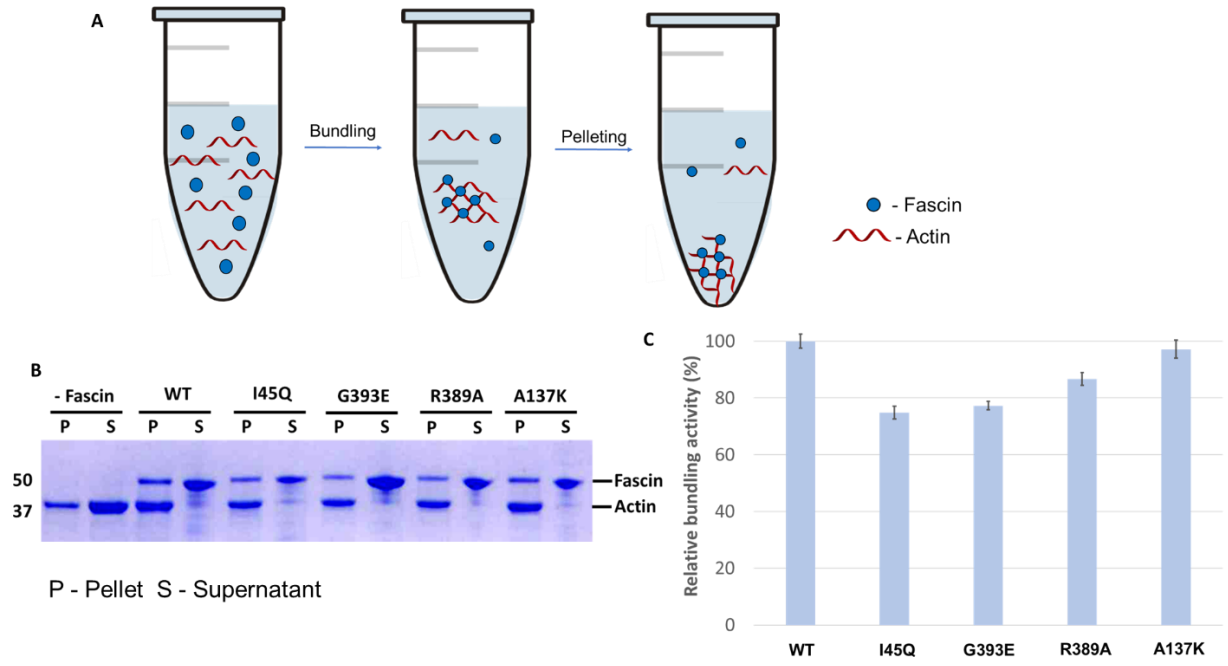

Figure 4.3: Slow-speed actin pelleting assay. A) Schematic showing the polymerization of actin. Fascin bundles free F-actin. Once bundles are formed, the fascin-actin complex can be pelleted. B) Coomassie stain of the pellets (P) and supernatants (S) of actin incubated with and without fascin proteins. C) Quantification of relative actin bundling activity.

Previous results in the Yang lab show that BTA-EG_4 does not inhibit fascin's actin bundling activity (unpublished results). The same trend was observed with BTA-EG_6 as actin bundling appeared unaffected when fascin was incubated with BTA-EG_6 (Figure 4.4-A). Actin pelleted similar to the fascin samples that were not treated with any compound (Figure 4.4-B). As a positive control, I used G2 (a known fascin inhibitor) for the actin bundling assay. The results

show that the actin bundling activity of fascin and fascin mutant proteins was greatly diminished in the presence of G2 (Figure 4.4-C, D). These data provide further evidence that though both BTA-EG$_6$ and G2 bind to fascin, they are mechanistically different.

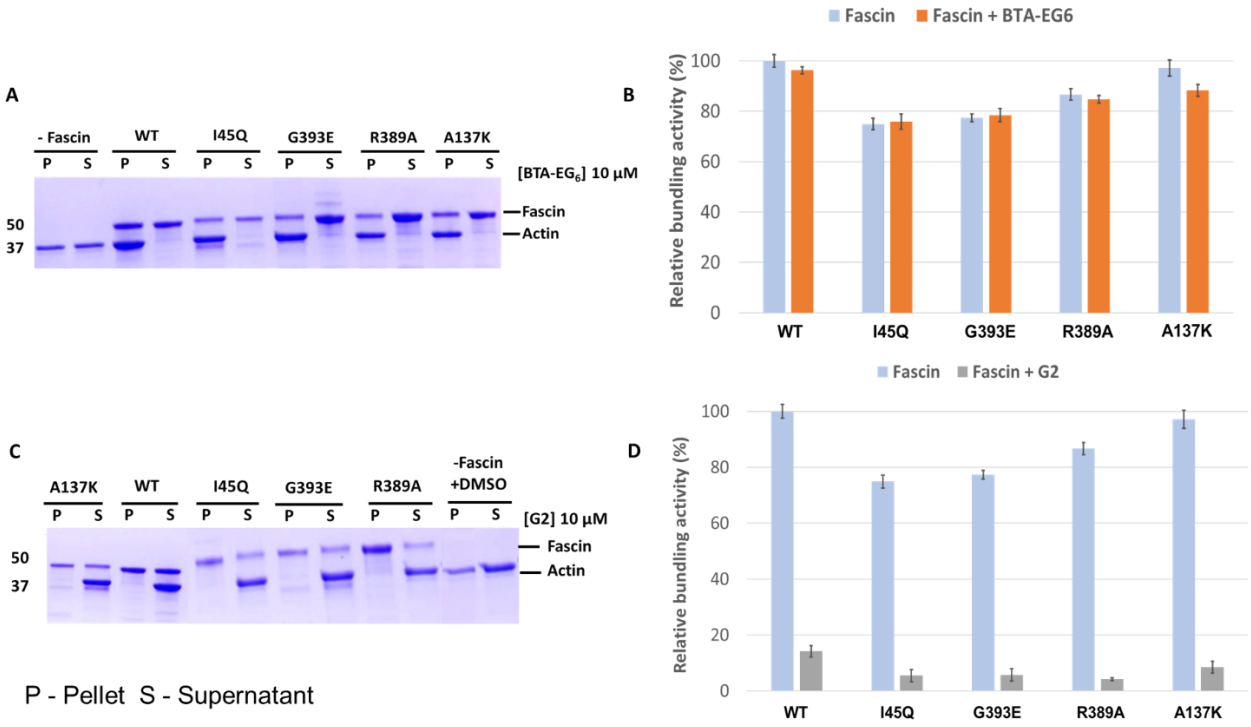

Figure 4.4: A) Coomassie stain of the pellets (P) and supernatants (S) of actin sedimentation assay with 10 µM BTA-EG$_6$. B) Quantification of relative actin bundling activity upon incubation with 10 µM BTA-EG$_6$. C) Coomassie stain of the pellets (P) and supernatants (S) of actin sedimentation assay with 10 µM G2 D) Quantification of relative actin bundling activity upon incubation with 10 µM G2.

4.5 Isothermal Titration Calorimetry

Evidence from competition photoaffinity labeling experiments, carried out previously in the Yang lab, suggested that BTA-EG$_4$ binds to fascin. To quantify and confirm that BTA-EG$_6$ indeed directly binds to fascin, I used the isothermal titration calorimetry (ITC) technique and measured the direct interaction of fascin and the small molecule. ITC is a direct measurement of the heat generated or absorbed when molecules interact. It is used to determine the thermodynamic

parameters of interactions of molecules (most often between small molecules and proteins) in solution[88].

Only BTA-EG_6 was tested due to the poor solubility of BTA-EG_4 in ITC experiments. The experimental raw data measures the heat release (or absorption) upon injecting a known amount of ligand into a known amount of protein[89]. Each injection therefore corresponds to a release of heat (visualized as a spike which over time returns to the baseline). These spikes are then integrated with respect to time. The data is analyzed as a function of the molar ration [BTA-EG_6]/[fascin] and allows us to acquire thermodynamic parameters of the interaction[89]. ITC data revealed that BTA-EG_6 directly interacts with and binds to WT-fascin with a 1:1 ratio and a K_d of 4.86 ± 0.07 μM. The binding was found to be exothermic (ΔH = -20.9 ± 1.77 kJ/mol) and involved an increase in entropy (31.8 ± 7.2 J/mol·K) (Figure 4.5).

Similar experiments were conducted for all the fascin mutant proteins using the same ligand and protein concentrations (Figure 4.6-4.9). As compared to the results obtained for wildtype fascin and BTA-EG_6, an increase in binding was obtained with mutants A137K and I45Q and a decrease in binding was observed for mutants R389A and G393E (Table 4.1).

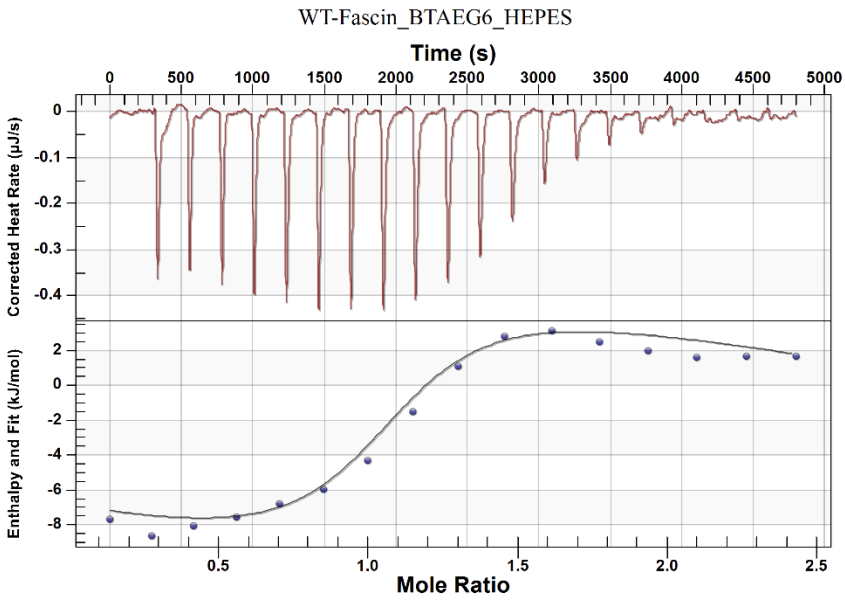

Figure 4.5: Representative example of a binding isotherm of titration between 1mM BTA-EG_6 and 100 µM wildtype Fascin.

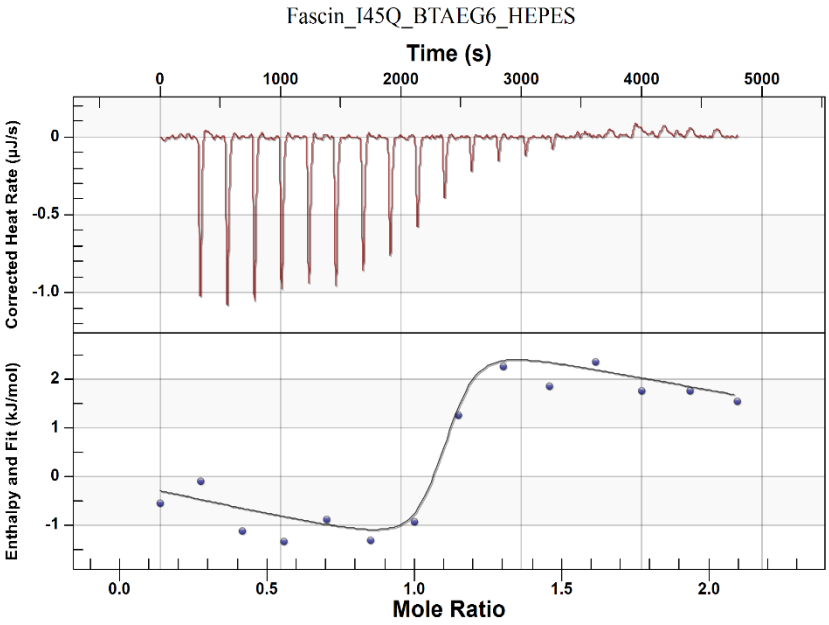

Figure 4.6: Representative example of a binding isotherm of titration between 1mM BTA-EG_6 and 100 µM Fascin-I45Q mutant.

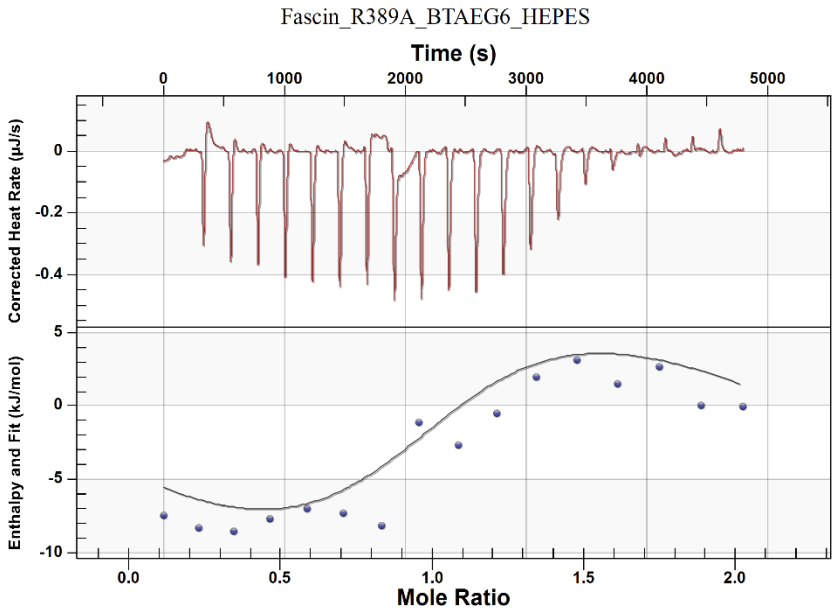

Figure 4.7: Representative example of a binding isotherm of titration between 1mM BTA-EG_6 and 100 µM Fascin-R389A mutant.

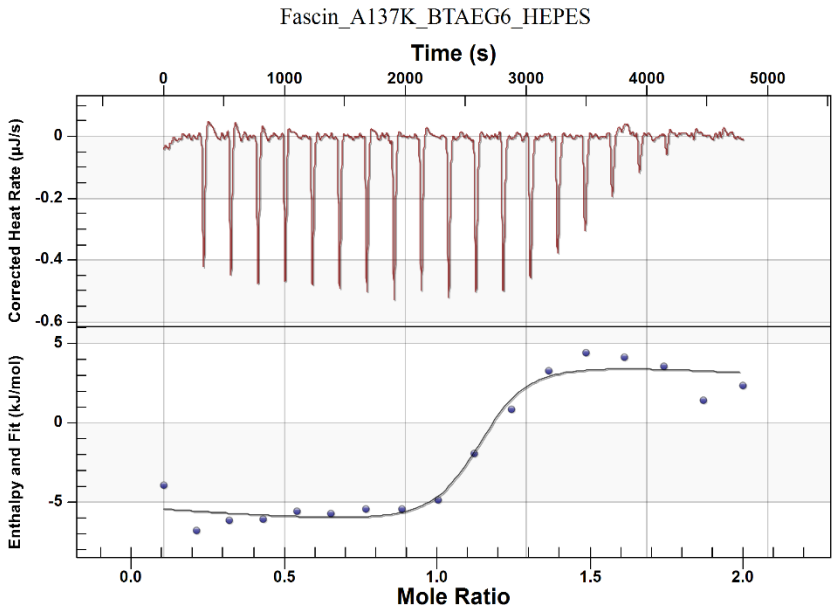

Figure 4.8: Representative example of a binding isotherm of titration between 1mM BTA-EG_6 and 100 µM Fascin-A137K mutant.

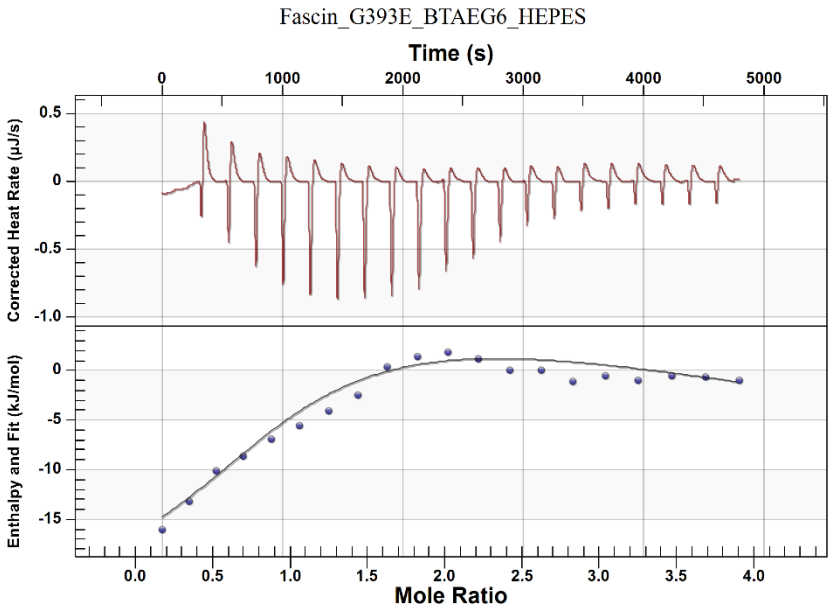

Figure 4.9: Representative example of a binding isotherm of titration between 1mM BTA-EG_6 and 100 µM Fascin-G393E mutant.

Table 4.1: ITC Data

	Kd(µM) *	**ΔH (kJ/mol)***	**ΔS(J/mol.K)***	**ΔG(kJ/mol)* = (ΔH – TΔS)**	**N***
WT-Fascin	4.86 ± 0.072	-20.9 ± 1.77	31.8 ± 7.20	-30.37 ± 3.91	1.05 ± 0.023
A137K	0.75 ± 0.03	-11.6 ± 0.238	78.5 ± 1.15	-34.99 ± 0.58	1.09 ± 0.008
I45Q	0.30 ± 0.07	-5.61 ± 0.977	107 ± 5.363	-37.49 ± 2.57	1.03 ± 0.013
R389A	14.0 ± 2.51	-39.3 ± 2.92	-38.5 ± 8.67	-27.8 ± 5.5	1.04 ± 0.06
G393E	36.8 ± 3.37	-43.7 ± 3.44	-61.5 ± 12.23	-25.37 ± 7.08	1.05 ± 0.043

*average from triplicates

4.6 Discussion

In this chapter, I characterized the binding interaction between BTA-EG_6 and fascin by using site-directed mutagenesis. I expressed recombinant wildtype and mutant fascin proteins for subsequent experiments. First, I performed the actin bundling activity assay using BTA-EG_6. The results demonstrated that BTA-EG_6 does not affect bundling activity of fascin or fascin mutant proteins. The folding of wildtype and mutant fascin proteins was assessed using circular dichroism spectroscopy. The spectra of all the mutant proteins aligned well with that observed for the wildtype. To characterize the binding quantitatively, isothermal titration calorimetry (ITC) was employed. ITC data revealed that BTA-EG_6 directly interacts with fascin. This binding was found to be in the micromolar range and the interaction was found to be exothermic. Table 4.1 lists the thermodynamic parameters obtained from the ITC experiment performed using wildtype and fascin mutant proteins. This data revealed that mutation in the protein affected its binding affinity with the ligand.

The present data suggests that binding of BTA-EG_6 to fascin affects the overall entropy of the process. Data from the binding curves of fascin mutants A137K and I45Q revealed increased entropy with an overall improved binding affinity. The increased entropy could be attributed to the release of bound water molecules from the binding cleft to the bulk solvent. On the contrary, data for R389A fascin mutant suggested a loss of entropy and an overall reduced binding affinity. This observation is consistent with the opposite result achieved in the case of fascin mutants, A137K and I45Q, by decreasing the hydrophobic interactions in the binding site and hence, increasing solvent accessibility. An interesting result was obtained in the case of fascin mutant G393E, where an increase in hydrophilicity in the binding site was accompanied by a decrease in entropy and an overall decreased association constant. Based on these observations, it can be

hypothesized that there is another point of interaction which is stabilizing trefoils 1 and 4 and in turn, affecting the binding affinity. Initially, E390 is interacting with the loop of lysine residues present in trefoil 1 (Figure 4.10). This interaction has a positive stabilizing effect on the binding cleft. Now, the mutation G393E enhances this interaction and stabilizes the binding pocket further (Figure 4.10). As a consequence, the binding site takes up a more 'closed' form and is less solvent accessible, reducing the overall entropy. Similarly, due to steric interactions, R389 keeps the binding pocket in an 'open' conformation. Mutating R389A disrupts this interaction and the pocket achieves a more 'closed' form. As seen previously, less solvent is being displaced resulting in more order and diminished entropy. Further evidence can be provided for this hypothesis involving a new point of interaction by making double mutations in trefoils 1 & 4.

The *in silico* model together with the biochemical data supports the participation of residues Ala137, Gly393, Ile45 and Arg389 in the binding mode of BTA-EG_6 to fascin.

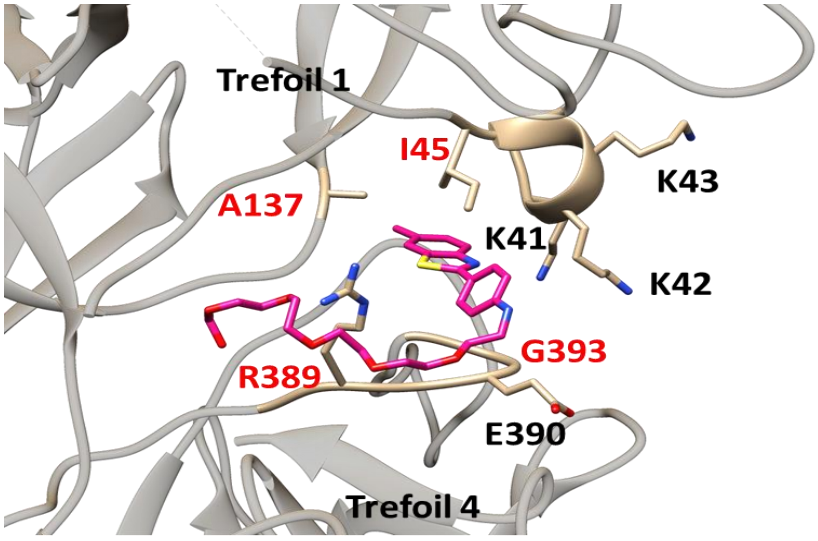

Figure 4.10: Hypothesis for stabilizing effect between trefoils 1 and 4 - the lysine residues on trefoil 1 have a stabilizing effect on the binding pocket, regulating the solvent accessibility. The mutation G393E enhances this interaction and stabilizes the pocket. Similarly, mutation R389A disrupts the interaction that was keeping the pocket in an "open" form, having the same effect as seen with G393E.

4.7 Conclusions

The mechanism of BTA-$EG_{4/6}$ induced spinogenesis remains elusive. Previous studies in the Yang lab revealed the cellular target of BTA-EG_4 to be fascin. To help address the gaps in knowledge behind the phenotypic activity of BTA compounds, this work provides preliminary data for a possible binding site of BTA-EG_6 to fascin. In order to obtain insight into the binding reaction, we used *in silico* methods to propose a binding site for the fascin-BTA-EG_6 complex. Mutational analysis and biochemical assays were carried out to investigate the proposed binding site. Current microcalorimetric results obtained confirmed the direct interaction of wildtype fascin with BTA-EG_6. ITC data shows that we were able to increase and decrease the binding of BTA-EG_6 to fascin by an order of magnitude. This result was achieved by introducing specific point mutations in the binding site. The change in entropy observed with fascin and fascin mutant proteins could be attributed to the release of water molecules from the binding cleft to the bulk solvent. Our data provides a basis for designing specific ligands to target the binding site.

Future work can involve developing more potent inhibitors of fascin activity. This can be achieved by designing molecules that increase the hydrophobic interactions in the binding pocket without compromising the entropy. Further, making double and triple mutations can provide support for the binding pocket of BTA molecules in this thesis. Similarly, single molecule FRET (Fluorescence Resonance Energy Transfer) analysis of Fascin-BTA-EG_6 can be employed to support the evidence obtained in this thesis. In the FRET measurements, the extent of non-radiative energy transfer between the donor and acceptor molecules (both fluorescently dyed), reports the intervening distance between them[90].

Previous results in the Yang lab suggest that BTA-EG_4 inhibits the interaction between fascin and Rab35. BTA-EG_6 can be used to replicate these results followed by studying their

interactions using FRET or microscopy. Fascin and Rab35 can be expressed with fluorescent tags. If there is binding, it should result in a FRET signal. If BTA abolishes this interaction (as seen previously), the FRET signal should reduce/ disappear[90]. Confirming that binding of BTA to Fascin is related to the phenotypic effect would be a challenging feat. The idea would be to develop a fascin mutant that bundles actin and is functional but cannot bind to Rab35. This mutant protein can then be expressed in primary neurons to see the effects on dendritic spine density. If the fascin mutant shows phenocopy effect of BTA-$EG_{4/6}$, it would validate the model for BTA induced spinogenesis (Figure 2.6).

4.8 Methods

General SDS-PAGE and Western Blotting Protocol

Samples were treated with 4X LDS sample buffer (Novex) and were heated at 95°C for 10 min. Twenty-microliters of sample were loaded onto a NuPAGE Novex 4-12% Bis-tris gel (ThermoFisher). The gel was run at 200V in NuPAGE MOPS SDS running buffer (ThermoFisher) for approximately 45 min. If required, the proteins were transferred onto a 0.45 μm nitrocellulose blot (ThermoFisher). Transfer occurred at 10V in a tris-glycine buffer (25 mM Tris, 20 mM glycine) for 1 h. The blot was blocked in blocking buffer (20 mM Tris, 125 mM NaCl, 0.1% Tween 20, 5% BSA) for 1 h at RT. Blots were incubated with a primary antibody diluted in blocking buffer overnight at 4°C. Blots were washed 5 times in wash buffer (TBS + 0.1% Tween 20). If necessary, blots were incubated with a secondary antibody diluted in blocking buffer for 1 h at RT and were washed just as previously mentioned. Blots were developed with Amersham ECL Western Blotting Detection Reagent (GE Healthcare Life Sciences).

Expression and Purification of Recombinant Wildtype Fascin

Recombinant human fascin 1 was expressed as a glutathione-S-transferase (GST) fusion protein in BL21(DE3) *Escherichia coli* cells using a pGEX-5x-2 vector. The transformed bacteria were plated onto LB Amp-100 agar plates and incubated overnight at 37°C. The next day, a freshly grown colony was used to inoculate ~20 mL 2XYT Amp-100 broth and incubated overnight at 37°C with stirring (180-200 r.p.m).

The next day, 1L 2XYT Amp-100 broth was inoculated with approximately 10 mL overnight culture. The culture was grown at 37°C until attenuance at 600 nm (OD_{600}) reached ~0.8. The culture was then transferred to 17°C and fascin expression was induced with 0.5 mM isopropyl β-D-thiogalactoside (IPTG)(Teknova) for 16 h.

After induction, the bacteria were harvested by centrifugation at 4000xg for 20 min. The pellets were suspended in 30 ml of Tris-HCl (20 mM Tris-HCl, pH 8.0, 150 mM NaCl) supplemented with 0.2 mM phenylmethylsulphonyl fluoride (PMSF), 1 mM dithiothreitol (DTT), 1 % Triton X-100 and 1 mM EDTA.

After sonication, the suspension was centrifuged at 15,000 r. p.m. for 30 min to remove the cell debris. The supernatant was then incubated for 3 h with 4 ml of glutathione beads (Sigma) at 4°C. After extensive washing with Tris-HCl (20 mM Tris-HCl pH 8.0, 150 mM NaCl), the beads were resuspended in 10 ml of thrombin cleavage buffer (20 mM Tris-HCl, pH 8.0, 150 mM NaCl, 2 mM CaCl2, 1 mM DTT). Fascin was released from the beads by incubation overnight with 40–100 U of thrombin at 4°C. After centrifugation, 0.2 mM phenylmethylsulphonyl fluoride (PMSF) was added to the supernatant to inactivate the remnant thrombin activity. The fascin protein was further concentrated with Amicon 10 MWCO protein concentrator (Millipore) to about

15 mg ml^{-1}. The purity of the recombinant fascin was determined by SDS-PAGE and the identity was confirmed by western blot using anti-fascin antibody.

Site-directed Mutagenesis of Human Fascin

Q5®Site-directed mutagenesis kit (NEB) was used to introduce point mutations. Both forward and reverse primers for specific mutations were designed using the online NEBaseChanger software (Table 4.2). PCR was carried out using standard conditions (Table 4.3). The identity of insert was checked by DNA sequencing. The same protocol for expression and purification as that for wildtype fascin mentioned above was followed. Protein purity was assessed visually by gel electrophoresis and Coomassie brilliant blue stain, and protein identity was confirmed by western blot using an anti-fascin antibody.

Table 4.2: Forward (-F) and reverse (-R) primers used for point mutations in wildtype Fascin

Primer	**Sequence***	**Length (nt)**
A137K_F	CGTGCACATC**AAG**ATGCACCCTC	23
A137K_R	CTCCACTTCTCGGCGGGG	18
I45Q_F	GAAGAAGCAG**CAG**TGGACGCTGG	23
I45Q_R	TTCAGGCTGCTGGCGGAC	18
R389A_F	CATCGTGTTC**GCA**GGGGAGCATG	23
R38A_R	ATGGGGCGGTTGATGAGCTTCATG	24
G393E_F	GGGGAGCATG**AAT**TCATCGGCTG	23
G393E_R	GCGGAACACGATGATGGG	17

*mutated or inserted nucleotides are shown in bold

Table 4.3: PCR reaction components

	Reaction Mix	Final Concentration
Q5 Hot Start High-Fidelity 2X Master Mix	12.5 µl	1X
10 µM Forward Primer	1.25 µl	0.5 µM
10 µM Revers Primer	1.25 µl	0.5 µM
Template Plasmid DNA (1-25 ng/µl)	1 µl	1-25 ng
Nuclease-free water	9.0 µl	
Final Volume	25 µl	

Circular Dichroism

CD spectra of wildtype and mutant fascin proteins were collected in the range of 195-300 nm using a Jasco J-810 spectropolarimeter. All the samples were prepared in tris buffer (2 mM Tri [pH 7.4], 1 mM DTT, 2 mM $MgCl_2$) and the experiments were performed at 25°C. The CD spectra were normalized with respect to protein concentration (0.5 µM) and the pathlength of the cuvette used (0.1 cm).

Molar ellipticity was calculated using the following formula and averaged across 3 scans -

$$[\theta](molar\ ellipticity) = MW \times 100 \times \theta / c \times d\ (deg \cdot cm^2 \cdot dmol^{-1})(c\ in \frac{mg}{ml}; d\ in\ cm)$$

$$[\theta](mean\ residue\ ellipticity) = MRW \times \theta / 10c \times d\ (deg.cm^2.dmol^{-1})$$

$$MRW\ (mean\ residue\ weight) = M/(N-1)\ (approx. 110 \pm 5\ Da)$$

Slow speed actin sedimentation assay

F-Actin bundling activity was measured by a low-speed centrifugation assay. This actin polymerization assay was adapted from the work of Huang and coworkers[85]. In the low-speed centrifugation assay, monomeric rabbit G-actin (Cytoskeleton, Inc) was induced to polymerize at room temperature in F-actin buffer (20 mM Tris-HCl, pH 8, 1 mM ATP, 1 mM DTT, 2 mM MgCl2, and 100 mM KCl) to a final concentration of 2 μM. Recombinant fascin proteins (wild-type or mutant) were dissolved in polymerization buffer (2mM Tris, 1 mM ATP, 1mM DTT, 2mM $MgCl_2$, 100 mM KCl, pH 8.0) to a final concentration of 0.5 μM. BTA-EG_6 or G2 (with 1% DMSO) (Xcessbio Biosciences) were both dissolved in polymerization buffer to a final concentration of 10 μM. Equal volumes of fascin solution were subsequently incubated with F-actin for 60 min at room temperature and centrifuged for 30 min at 10,000 g in an Eppendorf 5415D table top centrifuge.

Both supernatants and pellets were dissolved in an equivalent volume of SDS sample buffer (Novex) and the amount of actin was determined by SDS-PAGE. I measured the intensities of fascin proteins in Coomassie-stained gels and then calculated the relative actin-bundling activity, P, by the following formula: $P= 100 \times M_p/M_{pc}$, where P is the relative actin-bundling activity, M_p is the percentage of actin present in pellet when mixed with different concentrations of fascin protein, calculated by (intensity in pellet)/(intensity in pellet + intensity in supernatant), and M_{pc} is the percentage of actin that is present in pellet when mixed with WT fascin used as a control for the experiment.

Isothermal titration calorimetry

Calorimetric measurements were carried out using a Low Volume ITC instrument from TA Instruments. In each experiment, the ligand was titrated to the protein solution present in the 350 µl sample cell. The reference cell contained double-distilled water. All measurements were carried out at 25°C. The protein was dialyzed in 50 mM HEPES buffer (pH 7.5), 150 mM NaCl to a concentration of 100 µM. Protein concentrations were determined by Nanodrop ultraviolet spectrophotometer. The ligand solution contained 1 mM of the small molecule dissolved in the same buffer as the protein. Solutions were degassed at 25°C under vacuum for 60 min.

Upon experimental setup, the protein solution present in the sample cell was stirred at 180 r.p.m. After a stable baseline had been achieved, the titration was initiated. The injection sequence composed 20 injections of 2.5 µl in time intervals of 180 s until complete saturation was obtained. Heat changes caused by each ligand injection were obtained from the integral of the calorimetric signal. Data were analyzed using the NanoAnalyze software (TA Instruments) for fitting points to the independent binding model. Experimental heats of the protein-inhibitor titration were corrected for heats of dilution. All measurements were carried out at least in triplicates. Given energy values, binding constants and standard deviations were derived from data fitting and subsequent averaging of the corresponding measurements. Standard Gibbs free energy values were calculated using the equation ΔG_0=-RTlnK_b (where R=8.3144 J mol^{-1} K^{-1}, K_b binding constant).

Protein Modeling

Crystallographic structure of fascin was retrieved from the RCSB Protein Data Bank, PDB ID: 1DFC[2]. The protein was modeled using Protein preparation wizard[91] of Schrodinger suite; the protein structure was prepared by adding hydrogen atoms, optimizing hydrogen bonds and verifying the protonation states of His, Gln and Asn. Energy minimization was carried out using the default constraints of 0.3 Å RMSD and OPLS 2005 force field.

Ligand Preparation

For ligand preparation, a high quality, all atom 3-D structure of BTA-EG_6 was constructed in Maestro[92]. Schrodinger ligand preparation product, LigPrep[93] was used to prepare the ligand for molecular docking. The ligand preparation included 2D–3D conversions, generating variations, correction, verification and optimization of the structures.

Molecular Docking

The amino acids in the selected binding region were 22, 27, 29, 39, 41, 68, 398, 408, 471, 488. A receptor grid was generated using receptor grid generation in the Glide application[94] of Maestro[92]. The receptor grid for fascin was generated by specifying the binding site residues and was made to be large enough to contain the binding site of the protein and significant regions of the surrounding surface for effective binding. Glide docking tool of Schrodinger was used to dock the ligand to fascin protein and the ligand docking calculations were done on extra precision (XP) mode on Glide[94]. The docked conformers were evaluated using Glide (G) Score. The G Score is calculated as follows:

$$G\ Score = a * vdW + b * Coul + Lipo + Hbond + Metal + BuryP + RotB + Site$$

Wherein vdW denotes van der Waals energy, Coul denotes Coulomb energy, Lipo denotes lipophilic contact, HBond indicates hydrogen-bonding, Metal indicates metal-binding, BuryP indicates penalty for buried polar groups, RotB indicates penalty for freezing rotatable bonds, Site denotes polar interactions in the active site and a=0.065 and b=0.130 are coefficients of vdW and Coul.

Multiple independent docking runs generated 30 poses for the ligand with different conformations at the binding site. Next, these poses were clustered together using cutoff RMSD value of 2 Å. 10 different clusters were obtained as a result. Ligand interaction tool of Maestro (Schrodinger) was used to study the expected interactions between ligand and protein residues in the binding site. Poses with top scores exhibited hydrogen bonding interaction with amino acids present in the binding pocket. A representative pose with the highest docking score from the most favored cluster of poses was chosen which establishes the interactions between the ligand and protein residues in the binding site.

REFERENCES

(1) Alzheimer's Disease Facts and Figures. *Alzheimer's Assoc.* **2018**, *14(3)*, 367–429.

(2) Sedeh, R. S.; Fedorov, A. A.; Fedorov, E. V.; Ono, S.; Matsumura, F.; Almo, S. C.; Bathe, M. Structure, Evolutionary Conservation, and Conformational Dynamics of Homo Sapiens Fascin-1, an F-Actin Crosslinking Protein. *J.Mol.Biol.* **2010**, *400*, 589–604.

(3) Zhang, J.; Fonovic, M.; Suyama, K.; Bogyo, M.; Scott, M. P. Rab34 Controls Actin Bundling by Recruiting Fascin as an Effector Protein. *Science (80-.).* **2009**, *325*, 1250.

(4) Brunnstrom, H. R.; Englund, E. M. Cause of Death in Patients with Dementia Disorders. *Eur. J. Neurol.* **2009**, *16* (4), 488–492.

(5) Kochanek, K. D.; Murphy, S. L.; Xu, J.; Tejada-Vera, B. *National Vital Statisitcs Reports, Volume 65, Number 4*; 2014; Vol. 65.

(6) Hasselmo, M. E. The Role of Acetylcholine in Learning and Memory. *Curr. Opin. Neurobiol.* **2009**, *16* (6), 710–715.

(7) Francis, P. T.; Palmer, A. M.; Snape, M.; Wilcock, G. K. The Cholinergic Hypothesis of Alzheimer 's Disease : A Review of Progress. *J Neurol Neurosurg Psychiatry* **1999**, *66*, 137–147.

(8) Colovic, M. B.; Krsti, D. Z.; Lazarevic-Pasti, T. D.; Bondzic, A. M.; Vasic, V. M. Acetylcholinesterase Inhibitors : Pharmacology and Toxicology. *Curr. Neuropharmacol.* **2013**, *11*, 315–335.

(9) Raskind, M. A.; Peskind, E. R.; Wessel, T.; Yuan, W. Galantamine in AD A 6-Month Randomized , Placebo-Controlled Trial with a 6-Month Extension. *Neurology* **2000**, *54*, 2261–2268.

(10) Onor, M. L.; Trevisiol, M.; Aguglia, E. Rivastigmine in the Treatment of Alzheimer 's Disease : An Update. *Clin. Interv. Aging* **2007**, *2* (1), 17–32.

(11) Cacabelos, R. Donepezil in Alzheimer's Disease : From Conventional Trials to Pharmacogenetics. *Neuropsychiatr. Dis. Treat.* **2007**, *3* (3), 303–333.

(12) Walton, H. S.; Dodd, P. R. Glutamate – Glutamine Cycling in Alzheimer's Disease. *Neurochem. Int.* **2007**, *50*, 1052–1066.

(13) Masliah, E.; Alford, M.; Deteresa, R.; Mallory, M.; Hansen, L. Deficient Glutamate Transport Is Associated with Neurodegeneration in Alzheimer's Disease. *Ann Neurol* **1996**, *40* (5), 759–766.

(14) Danysz, W.; Parsons, C. G. The NMDA Receptor Antagonist Memantine as a Symptomatological and Neuroprotective Treatment for Alzheimer's Disease : Preclinical

Evidence. *Int J Geriatr Psychiatry* **2003**, *18*, S23–S32.

(15) Casey, D. A.; Antimisiaris, D.; Brien, J. O. Drugs for Alzheimer's Disease : Are They Effective ? *P&T* **2010**, *35* (4), 208–211.

(16) FDA-Approved Treatents for Alzheimer's. *Alzheimer's Association*. 2017.

(17) Folch, J.; Petrov, D.; Ettcheto, M.; Abad, S.; Sánchez-lópez, E.; García, M. L.; Olloquequi, J.; Beas-zarate, C.; Auladell, C.; Camins, A. Current Research Therapeutic Strategies for Alzheimer's Disease Treatment. *Neural Plast.* **2016**, *2016*, 15.

(18) Gotz, J.; Gotz, N. N. Animal Models for Alzheimer's Disease and Frontotemporal Dementia : A Perspective. *ASN Neuro* **2009**, *1* (4), 251–264.

(19) Perl, D. P. Neuropathology of Alzheimer's Disease. *Mt Sinai J Med* **2010**, *77* (1), 32–42.

(20) Murphy, M. P.; LeVine III, H. Alzheimer's Disease and the β-Amyloid Peptide. *J Alzheimers Dis* **2010**, *19* (1), 311.

(21) Beta-Amyloid and the Amyloid Hypothesis. *Alzheimer's Assoc.* **2017**.

(22) Lorenzo, A.; Yankner, B. A. β-Amyloid Neurotoxicity Requires Fibril Formation and Is Inhibited by Congo Red. *Proc. Natl. Acad. Sci.* **1994**, *91*, 12243–12247.

(23) Perry, G.; Cash, A. D.; Smith, M. A. Alzheimer Disease and Oxidative Stress. *Biomed. Biotechnol.* **2002**, *3*, 120–123.

(24) Carson, J. A.; Turner, A. J. B -Amyloid Catabolism : Roles for Neprilysin (NEP) and Other Metallopeptidases? *Neurochemistry* **2002**, *81*, 1–8.

(25) Butterfield, D. A.; Swomley, A. M. Amyloid β-Peptide (1-42)-Induced Oxidative Stress in Alzheimer Disease: Importance in Disease Pathogenesis and Progression. *Therapeutics* **2013**, *19* (8).

(26) Habib, L. K.; Lee, M. T. C.; Yang, J. Inhibitors of Catalase-Amyloid Interactions Protect Cells from β-Amyloid-Induced Oxidative Stress and Toxicity. *Biol. Chem.* **2010**, *285* (50), 38933–38943.

(27) Inbar, P.; Li, C. Q.; Takayama, S. A.; Bautista, M. R.; Yang, J. Oligo (Ethylene Glycol) Derivatives of Thioflavin T as Inhibitors of Protein – Amyloid Interactions. *ChemBioChem* **2006**, *7*, 1563–1566.

(28) Biancalana, M.; Koide, S. Molecular Mechanism of Thioflavin-T Binding to Amyloid Fibrils. *Biochim Biophys Acta.* **2010**, *1804* (7), 1405–1412.

(29) Inbar, P.; Yang, J. Inhibiting Protein – Amyloid Interactions with Small Molecules : A Surface Chemistry Approach. *Bioorg. Med. Chem. Lett* **2006**, *16*, 1076–1079.

(30) Klunk, W. E.; Wang, Y.; Huang, G.; Debnath, M. L.; Holt, D. P.; Mathis, C. A.

Uncharged Thioflavin-T Derivatives Bind to Amyloid-Beta Protein with High Affinity and Readily Enter the Brain. *Life Sci.* **2001**, *69*, 1471–1484.

(31) Min, J.; Marie, A.; Me, Y.; Myung, J.; Turner, R. S.; Yang, J.; Pak, D. T. S.; Lee, H.; Hoe, H. A Tetra (Ethylene Glycol) Derivative of Benzothiazole Aniline Ameliorates Dendritic Spine Density and Cognitive Function in a Mouse Model of Alzheimer's Disease. *Exp. Neurol.* **2014**, *252*, 105–113.

(32) Lee, N. J.; Song, J. M.; Cho, H. J.; Sung, Y. M.; Lee, T.; Chung, A.; Hong, S. H.; Cifelli, J. L.; Rubinshtein, M.; Habib, L. K.; Capule, C. C; Turner, R.S; Pak, D.T.S; Yang,J; Hoe, H. S. Hexa (Ethylene Glycol) Derivative of Benzothiazole Aniline Promotes Dendritic Spine Formation through the RasGRF1-Ras Dependent Pathway. *Biochim. Biophys. Acta - Mol. Basis Dis.* **2016**, *1862* (2), 284–295.

(33) Rochefort, N. L.; Konnerth, A. Dendritic Spines: From Structure to in Vivo Function. *EMBO Rep.* **2012**, *13* (8), 699–708.

(34) Hering, H.; Sheng, M.; Medical, H. H. DENDRITIC SPINES : STRUCTURE , DYNAMICS AND REGULATION. *Neuroscience* **2001**, *2*, 880–888.

(35) Hotulainen, P.; Hoogenraad, C. C. Actin in Dendritic Spines : Connecting Dynamics to Function. *J. Cell Biol.* **2010**, *189* (4), 619–629.

(36) Leuner, B.; Falduto, J.; Shors, T. J. Associative Memory Formation Increases the Observation of Dendritic Spines in the Hippocampus. *J. Neurosci* **2003**, *23* (2), 659–665.

(37) Collin, C.; Miyaguchi, K.; Segal, M.; Miyaguchi, K.; Segal, M. Dendritic Spine Density and LTP Induction in Cultured Hippocampal Slices. *Physiology* **2019**, 1614–1623.

(38) Roberts, T. F.; Tschida, K. A.; Klein, M. E.; Mooney, R. Rapid Spine Stabilization and Synaptic Enhnacement at the Onset of Behavioural Learning. *Nature* **2010**, *463* (7283), 948–952.

(39) Xu, T.; Yu, X.; Perlik, A. J.; Tobin, W. F.; Zweig, J. A.; Jones, T.; Zuo, Y. Rapid Formation and Selective Stabilization of Synapses for Enduring Motor Memories. *Nature* **2010**, *462* (7275), 915–919.

(40) Segal, M. DENDRITIC SPINES AND LONG-TERM PLASTICITY. *Neuroscience* **2005**, *6*, 277–283.

(41) Spontaneous, S.; Engert, F.; Bonhoeffer, T. Dendritic Spine Changes Associated with Hippocampal Long-Term Synaptic Plasticity. *Nature* **1999**, *399*.

(42) Knobloch, M.; Mansuy, I. M. Dendritic Spine Loss and Synaptic Alterations in Alzheimer's Disease. *Mol Neurobiol* **2008**, *37*, 73–82.

(43) Penzes, P.; Cahill, M. E.; Jones, K. A.; VanLeeuwen, J.-E.; Woolfrey, K. M. Dendritic Spine Pathology in Neuropsychiatric Disorders. *Nat Neurosci.* **2012**, *14* (3), 285–293.

(44) Kane, R. E. Preparation and Purification of Polymerized Actin from Sea Urchin Egg Extracts. *Cell Biol.* **1975**, *66*, 305–315.

(45) Kane, R. E. Actin Polymerization and Interaction with Other Proteins in Temperature-Induced Gelation of Sea Urchin Egg Extracts. *Cell Biol.* **1976**, *71*, 704–714.

(46) J.J., O.; R.E., K.; J., B. Formation of Filopodia in Coelomocytes: Localization of Fascin, a 58 000 Dalton Actin Cross-Linking Protein. *Cell.* **1979**, *17*, 285–293.

(47) Yamashiro-Matsumura, S.; Matsumura, F. Purification and Characterization of an F-Actin-Bundling 55-Kilodalton Protein from HeLa Cells. *J. Biol. Chem.* **1985**, *260* (8), 5087–5097.

(48) Bryan, J.; Edwards, R.; Matsudaira, P.; Otto, J.; Wulfkuhle, J. Fascin, an Echinoid Actin-Bundling Protein, Is a Homolog of the Drosophila Singed Gene Product. *Proc. Natl. Acad. Sci.* **1993**, *90* (19), 9115–9119.

(49) Edwards, R. A.; Herrera-Sosa, H.; Otto, J.; Bryan, J. Cloning and Expression of a Murine Fascin Homolog from Mouse Brain. *Journal of Biological Chemistry*. 1995, pp 10764–10770.

(50) Holthuis, J. C. M.; Schoonderwoert, V. T. G.; Martens, G. J. M. A Vertebrate Homolog of the Actin-Bundling Protein Fascin. *Biochim. Biophys. Acta* **1994**, *1219*, 184–188.

(51) Tubb, B.; Mulholland, D. J.; Vogl, W.; Lan, Z. J.; Niederberger, C.; Cooney, A.; Bryan, J. Testis Fascin (FSCN3): A Novel Paralog of the Actin-Bundling Protein Fascin Expressed Specifically in the Elongate Spermatid Head. *Exp. Cell Res.* **2002**, *275* (1), 92–109.

(52) Han, S.; Huang, J.; Liu, B.; Xing, B.; Bordeleau, F.; Reinhart-King, C. A.; Li, W.; Zhang, J. J.; Huang, X. Y. Improving Fascin Inhibitors to Block Tumor Cell Migration and Metastasis. *Mol. Oncol.* **2016**, *10* (7), 966–980.

(53) Ono, S.; Yamakita, Y.; Yamashiro, S.; Matsudaira, P. T.; Gnarra, J. R.; Obinata, T.; Matsumura, F. Identification of an Actin Binding Region and a Protein Kinase C Phosphorylation Site on Human Fascin. *J. Biol. Chem.* **1997**, *272* (4), 2527–2533.

(54) Jansen, S.; Collins, A.; Yang, C.; Rebowski, G.; Svitkina, T.; Dominguez, R. Mechanism of Actin Filament Bundling by Fascin. *J. Biol. Chem.* **2011**, *286* (34), 30087–30096.

(55) Mattila, P. K.; Lappalainen, P. Filopodia: Molecular Architecture and Cellular Functions. *Nat. Rev. Mol. Cell Biol.* **2008**, *9* (6), 446–454.

(56) Vignjevic, D.; Kojima, S. I.; Aratyn, Y.; Danciu, O.; Svitkina, T.; Borisy, G. G. Role of Fascin in Filopodial Protrusion. *J. Cell Biol.* **2006**, *174* (6), 863–875.

(57) MacDonald, B. T.; Keiko, T.; He, X. Wnt/β-Catenin Signaling: Components, Mechanisms, and Diseases. *Dev Cell.* **2010**, *17* (1), 9–26.

(58) Clevers, H.; Nusse, R. Wnt/β-Catenin Signaling and Disease. *Cell* **2012**, *149* (6), 1192–1205.

(59) Valenta, T.; Hausmann, G.; Basler, K. The Many Faces and Functions of β-Catenin. *EMBO J.* **2012**, *31* (12), 2714–2736.

(60) Tao, Y. S.; Edwards, R. A.; Tubb, B.; Wang, S.; Bryan, J.; Mccrea, P. D. β-Catenin Associates with the Acctin-Bundling Protein Fascin in a Noncadherin Complex. *J. Cell Biol.* **1996**, *134* (5), 1271–1281.

(61) Scott, R. W.; Olson, M. F. LIM Kinases: Function, Regulation and Association with Human Disease. *J. Mol. Med.* **2007**, *85* (6), 555–568.

(62) Schwartz, M. Rho Signalling at a Glance. *J. Cell Sci.* **2004**, *117* (23), 5457–5458.

(63) Yang, N.; Higuchi, O.; Ohashi, K.; Nagata, K.; Wada, A.; Kangawa, K.; Nishida, E.; Mizuno, K. Cofflin Phosphorylation by LIM-Kinase 1 and Its Role in Rac-Mediated Actin Reorganization. *Nature* **1998**, *393* (6687), 809–812.

(64) Jayo, A.; Parsons, M.; Adams, J. C. A Novel Rho-Dependent Pathway That Drives Interaction of Fascin-1 with p-Lin-11/Isl-1/Mec-3 Kinase (LIMK) 1/2 to Promote Fascin-1/Actin Binding and Filopodia Stability. *BMC Biol.* **2012**, *10*, 1–19.

(65) Morley, S. C. The Actin-Bundling Protein L-Plastin: A Critical Regulator of Immune Cell Function. *Int. J. Cell Biol.* **2012**, *2012*, 935173.

(66) Kell, M. J.; Riccio, R. E.; Baumgartner, E. A.; Compton, Z. J.; Pecorin, P. J.; Mitchell, T. A.; Topczewski, J.; LeClair, E. E. Targeted Deletion of the Zebrafish Actin-Bundling Protein L-Plastin (Lcp1). *PLoS One* **2018**, *13* (1), 1–23.

(67) Van Audenhove, I.; Denert, M.; Boucherie, C.; Pieters, L.; Cornelissen, M.; Gettemans, J. Fascin Rigidity and L-Plastin Flexibility Cooperate in Cancer Cell Invadopodia and Filopodia. *J. Biol. Chem.* **2016**, *291* (17), 9148–9160.

(68) Chua, C. E. L.; Lim, Y. S.; Tang, B. L. Rab35 - A Vesicular Traffic-Regulating Small GTPase with Actin Modulating Roles. *FEBS Lett.* **2010**, *584* (1), 1–6.

(69) Bos, J. L.; Rehmann, H.; Wittinghofer, A. GEFs and GAPs: Critical Elements in the Control of Small G Proteins. *Cell* **2009**, *16* (3), 374–383.

(70) Chevallier, J.; Koop, C.; Srivastava, A.; Petrie, R. J.; Lamarche-Vane, N.; Presley, J. F. Rab35 Regulates Neurite Outgrowth and Cell Shape. *FEBS Lett.* **2009**, *583* (7), 1096–1101.

(71) Cohan, C. S.; Welnhofer, E. A.; Zhao, L.; Matsumura, F.; Yamashiro, S. Role of the Actin Bundling Protein Fascin in Growth Cone Morphogenesis: Localization in Filopodia and Lamellipodia. *Cell Motil. Cytoskeleton* **2001**, *48* (2), 109–120.

(72) Lowery, L. A.; Vactor, D. Van. The Trip of the Tip: Understanding the Growth Cone Machinery. *Nat Rev Mol Cell Biol.* **2009**, *10* (5), 332–343.

(73) Korobova, F.; Svitkina, T. Arp2/3 Complex Is Important for Filopodia Formation, Growth Cone Motility, and Neuritogenesis in Neuronal Cells. *Mol. Biol. Cell* **2008**, *19* (4), 1561–1574.

(74) Tan, V. Y.; Lewis, S. J.; Adams, J. C.; Martin, R. M. Association of Fascin-1 with Mortality, Disease Progression and Metastasis in Carcinomas: A Systematic Review and Meta-Analysis. *BMC Med.* **2013**, *11*, 52.

(75) Talmadge, J. E.; Fidler, I. J. The Biology of Cancer Metastasis: Historical Perspective. *Cancer Res.* **2010**, *70* (14), 5649–5669.

(76) Yamaguchi, H. Pathological Roles of Invadopodia in Cancer Invasion and Metastasis. *Eur. J. Cell Biol.* **2012**, *91* (11–12), 902–907.

(77) Machesky, L. M.; Lia., A. Fascin: Invasive Filopodia Promoting Metastasis. *Commun. Integr. Biol.* **2010**, *3* (3), 263–270.

(78) Nakae, K.; Yoshimoto, Y.; Sawa, T.; Homma, Y.; Hamada, M.; Takeuch, T.; Imoto, M. Migrastatin, a New Inhibitor of Tumor Cell Migration from Streptomyces Sp. MK929-43F1. Taxonomy, Fermentation, Isolation and Biological Activities. *J. Antibiot. (Tokyo).* **2000**, *53* (10), 1130–1136.

(79) Chanpimol, S.; Seamon, B.; Hernandez, H.; Harris-love, M.; Blackman, M. R. Migrastatin Analogues Target Fascin to Block Tumor Metastasis. *Nature* **2010**, *464* (7291), 1062–1066.

(80) Han, S.; Huang, J.; Liu, B.; Xing, B.; Bordeleau, F.; Reinhart-King, C. A.; Li, W.; Zhang, J. J.; Huang, X. Y. Improving Fascin Inhibitors to Block Tumor Cell Migration and Metastasis. *Mol. Oncol.* **2016**, *10* (7), 966–980.

(81) Huang, F. K.; Han, S.; Xing, B.; Huang, J.; Liu, B.; Bordeleau, F.; Reinhart-King, C. A.; Zhang, J. J.; Huang, X. Y. Targeted Inhibition of Fascin Function Blocks Tumour Invasion and Metastatic Colonization. *Nat. Commun.* **2015**, *6* (1), 7465.

(82) Kraft, R.; Kahn, A.; Medina-Franco, J. L.; Orlowski, M. L.; Baynes, C.; Lopez-Vallejo, F.; Barnard, K.; Maggiora, G. M.; Restifo, L. L. A Cell-Based Fascin Bioassay Identifies Compounds with Potential Anti-Metastasis or Cognition-Enhancing Functions. *Dis. Model. Mech.* **2013**, *6* (1), 217–235.

(83) Cui, M.; Mihaly, M.; Hong-Xing, Z.; Meng, X.-Y. Molecular Docking: A Powerful Approach for Structure-Based Drug Discovery. *Curr. Comput. Aided. Drug Des.* **2011**, *7* (2), 146–157.

(84) Mcconkey, B. J.; Sobolev, V.; Edelman, M. The Performance of Current Methods in Ligand–protein Docking. *Curr. Sci.* **2002**, *83* (7).

(85) Huang, J.; Dey, R.; Wang, Y.; Jakoncic, J.; Kurinov, I.; Huang, X. Y. Structural Insights into the Induced-Fit Inhibition of Fascin by a Small-Molecule Inhibitor. *J. Mol. Biol.* **2018**, *430* (9), 1324–1335.

(86) Clarke, D. T. Circular Dichroism and Its Use in Protein-Folding Studies. In *CD for Protein Folding*; Humana Press, Totowa, NJ, 2011; pp 59–72.

(87) Greenfield, N. J. Using Circular Dichroism Spectra to Estimate Protein Secondary Structure. *Nat. Protoc.* **2007**, *1* (6), 2876–2890.

(88) Freire, E.; Mayorga, O. L.; Straume, M. Isothermal Titration Calorimeter. *Anal. Chem.* **1990**, *62* (18), 950A–959A.

(89) The ITC Experiment; pp 1–7.

(90) Rahul, R.; Sungchul, H.; Taekjip, H. A Practical Guide to Single Molecule FRET. *Nat Methods.* **2013**, *5* (6), 507–516.

(91) Schrödinger. ProteinPrep | Schrödinger. *Schrödinger Release 2018-2*. 2018.

(92) L, S. Maestro, Version 9.1. *New York, NY*. **2010**.

(93) Schrödinger. LigPrep | Schrödinger. *Schrödinger Release 2018-2*. 2018.

(94) Schrödinger Llc New York Ny. Glide, Version 5.7. *Glide Schrödinger LLC NY*. 2011.